

# Choosing the Right Sea Surface Temperature Dataset: Benchmarking and Guidance for Climate Applications

Duo Chan<sup>a</sup>, Elizabeth C. Kent<sup>b</sup>, Nathan Lenssen<sup>c,d</sup>, Clara Deser<sup>d</sup>, Christopher J. Merchant<sup>e,f</sup>,  
Masayoshi Ishii<sup>g,h</sup>, Caroline Sandford<sup>i</sup>, Boyin Huang<sup>j</sup>, Xungang Yin<sup>j</sup>, John J. Kennedy<sup>k</sup>,  
Richard C. Cornes<sup>b</sup>, Peter Huybers<sup>l</sup>, Geoffrey Gebbie<sup>m</sup>

<sup>a</sup> *School of Ocean and Earth Science, University of Southampton, UK*

<sup>b</sup> *National Oceanography Centre, Southampton, UK*

<sup>c</sup> *Colorado School of Mines, Applied Mathematics and Statistics, USA*

<sup>d</sup> *National Center for Atmospheric Research, USA*

<sup>e</sup> *National Centre for Earth Observation, Reading, UK*

<sup>f</sup> *Department of Meteorology, University of Reading, Reading, UK*

<sup>g</sup> *Department of Climate and Geochemistry Research, Meteorological Research Institute, Japan  
Meteorological Agency, Tsukuba, Japan*

<sup>h</sup> *Geoenvironmental Sciences, University of Tsukuba, Tsukuba, Japan*

<sup>i</sup> *Met Office, Exeter, UK*

<sup>j</sup> *NOAA / National Centers for Environmental Information, North Carolina, USA*

<sup>k</sup> *Independent researcher, Verdun, France*

<sup>l</sup> *Department of Earth and Planetary Sciences, Harvard University, USA*

<sup>m</sup> *Department of Physical Oceanography, Woods Hole Oceanographic Institution, USA*

*Corresponding author: Duo Chan, Duo.Chan@soton.ac.uk*

21 ABSTRACT: Sea surface temperature (SST) datasets underpin many climate applications, includ-  
22 ing climate monitoring, the study of historical climate variability and change, attribution, model  
23 evaluation, ecosystem assessment, paleo-proxy calibration, and use as boundary conditions for  
24 atmospheric model simulations. Many different SST products are available. This paper addresses  
25 why SST products differ, what these differences mean for climate analyses, and which products  
26 are best suited for various purposes. Differences among SST products are first reviewed with  
27 respect to improvements in bias adjustments, gridding and infilling techniques, and uncertainty  
28 quantification. The implications of these advances are then assessed through historical case stud-  
29 ies, evaluation of spatial patterns, and comparison of global means and key regional indices.  
30 Substantial discrepancies in trends are found during the satellite era using older SST products, but  
31 recently-released datasets are much more consistent. Recent datasets also show a more-consistent  
32 SST evolution during World War II and in trends associated with Tropical Pacific zonal gradients.  
33 Disagreements persist, however, with respect to early-20<sup>th</sup>-century warming and in data-sparse  
34 regions such as the Southern Ocean and Arctic. To assist users across disciplines, we articulate  
35 principles for dataset selection based on application needs and highlight the NCAR Climate Data  
36 Guide and an accompanying web-based data-selector tool that provides updated benchmarking and  
37 access to SST products.

38 CAPSULE: A user-oriented synthesis of the evolution of sea surface temperature (SST) datasets,  
39 how their differences influence climate analyses, and practical guidance and tools to help users  
40 choose appropriate products.

## 41 **Significance Statement**

42 Sea surface temperature is an “Essential Climate Variable” used for tracking climate change,  
43 evaluating models, calibrating paleo-records, and understanding events such as marine heatwaves  
44 and El Niño. Many different datasets exist, produced by various scientific groups. In addition,  
45 there are multiple versions of many of these datasets, yet older versions remain in use long after  
46 improved versions have superseded them. This article explains how SST datasets have developed  
47 and improved, shows how differences between them can influence scientific results, and highlights  
48 where recent versions agree and where important uncertainties persist. Alongside a general  
49 encouragement to use up-to-date SST products, we offer practical, application-focused guidance  
50 as well as an online tool that helps researchers identify, understand, and access SST datasets  
51 well-suited to their needs, promoting proper, consistent use of sea surface temperature information.

## 52 **1. Introduction**

53 Sea surface temperature (SST) is a critical variable in climate science, providing the primary  
54 measure of ocean surface warming and a key indicator for monitoring climate change and variability.  
55 It informs analyses of marine heatwaves (Oliver et al. 2021), estimates of climate sensitivity  
56 (Sherwood et al. 2020), and attribution of observed changes to anthropogenic forcing (Eyring  
57 et al. 2023). SST also provides boundary conditions for atmospheric reanalyses (e.g. Hersbach  
58 et al. 2020; Kosaka et al. 2024), atmospheric model simulations, e.g., the Atmospheric Model  
59 Intercomparison Project (AMIP, Eyring et al. 2016), and represents key modes of climate variability  
60 such as the El Niño-Southern Oscillation (ENSO, McPhaden et al. 2006) and Atlantic Multidecadal  
61 Variability (AMV, Knight et al. 2006).

62 The SST datasets considered here are listed in Table 1 with acronyms defined and citation and  
63 access information. Each of these SST datasets generally target one of three main user requirements  
64 (Fig. 1):

TABLE 1: SST datasets used in this paper

Dataset	Dataset Name	Citation	Available from
DCSST	Dynamically Consistent SST	Chan et al. (2024a)	<a href="https://doi.org/10.7910/DVN/NU4UGW">https://doi.org/10.7910/DVN/NU4UGW</a>
DCSST-I	Dynamically Consistent SST - Infilled	Chan et al. (2026)	<a href="https://doi.org/10.7910/DVN/ROG38Q">https://doi.org/10.7910/DVN/ROG38Q</a>
HadSST4.2	Met Office Hadley Centre SST	Sandford and Rayner (2026)	<a href="https://www.metoffice.gov.uk/hadobs/hadsst4">https://www.metoffice.gov.uk/hadobs/hadsst4</a>
HadSST4.1		Kennedy et al. (2019)	<a href="https://www.metoffice.gov.uk/hadobs/hadsst4/previous_versions.html">https://www.metoffice.gov.uk/hadobs/hadsst4/previous_versions.html</a>
HadSST3		Kennedy et al. (2011a,b)	<a href="https://www.metoffice.gov.uk/hadobs/hadsst3">https://www.metoffice.gov.uk/hadobs/hadsst3</a>
HadSST2		Rayner et al. (2006)	<a href="https://www.metoffice.gov.uk/hadobs/hadsst2">https://www.metoffice.gov.uk/hadobs/hadsst2</a>
ERSSTv6	Extended Reconstructed SST	Huang et al. (2025)	<a href="https://www.ncei.noaa.gov/data/sea-surface-temperature-extended-reconstructed/v6/access/">https://www.ncei.noaa.gov/data/sea-surface-temperature-extended-reconstructed/v6/access/</a>
ERSSTv5		Huang et al. (2017)	<a href="https://www.ncei.noaa.gov/data/sea-surface-temperature-extended-reconstructed/v5/netcdf">https://www.ncei.noaa.gov/data/sea-surface-temperature-extended-reconstructed/v5/netcdf</a>
ERSSTv4		Huang et al. (2015)	<a href="https://www.ncei.noaa.gov/data/sea-surface-temperature-extended-reconstructed/v4/netcdf">https://www.ncei.noaa.gov/data/sea-surface-temperature-extended-reconstructed/v4/netcdf</a>
ERSSTv3b		Smith et al. (2008)	<a href="https://www.ncei.noaa.gov/data/sea-surface-temperature-extended-reconstructed/v3b/netcdf">https://www.ncei.noaa.gov/data/sea-surface-temperature-extended-reconstructed/v3b/netcdf</a>
COBE-SST3	Centennial in situ Observation-Based Estimates	Ishii et al. (2025)	<a href="https://climate.mri-jma.go.jp/pub/archives/Ishii-et-al_COBE-SST3/cobe-sst3">https://climate.mri-jma.go.jp/pub/archives/Ishii-et-al_COBE-SST3/cobe-sst3</a>
COBE-SST2		Hirahara et al. (2014)	<a href="https://climate.mri-jma.go.jp/pub/archives/Hirahara-et-al_COBE-SST2/">https://climate.mri-jma.go.jp/pub/archives/Hirahara-et-al_COBE-SST2/</a>
COBE-SST1		Ishii et al. (2005)	<a href="https://ds.data.jma.go.jp/tcc/tcc/products/el_nino/cobesst_doc.html">https://ds.data.jma.go.jp/tcc/tcc/products/el_nino/cobesst_doc.html</a>
HadISST1	Hadley Centre Sea Ice and Sea Surface Temperature data set	Rayner et al. (2003)	<a href="https://www.metoffice.gov.uk/hadobs/hadisst/">https://www.metoffice.gov.uk/hadobs/hadisst/</a>
COBE-SST3H	Centennial Observation-Based Estimates	Ishii et al. (2025)	<a href="https://climate.mri-jma.go.jp/pub/archives/Ishii-et-al_COBE-SST3/cobe-sst3h">https://climate.mri-jma.go.jp/pub/archives/Ishii-et-al_COBE-SST3/cobe-sst3h</a>
OISSTv2.1	Optimum Interpolation Sea Surface Temperature	Huang et al. (2021)	<a href="https://www.ncei.noaa.gov/products/optimum-interpolation-sst">https://www.ncei.noaa.gov/products/optimum-interpolation-sst</a>
OISSTv2		Reynolds et al. (2007, 2002)	<a href="https://www.ncei.noaa.gov/data/sea-surface-temperature-optimum-interpolation/v2">https://www.ncei.noaa.gov/data/sea-surface-temperature-optimum-interpolation/v2</a>
ESA SST3.0	European Space Agency Climate Change Initiative SST	Embury et al. (2024)	easy access: <a href="https://surftemp.net">https://surftemp.net</a> ; full global resolution: <a href="https://data.ceda.ac.uk/neodc/eocis/data/global_and_regional/sea_surface_temperature/CDR_v3/Analysis">https://data.ceda.ac.uk/neodc/eocis/data/global_and_regional/sea_surface_temperature/CDR_v3/Analysis</a>
CMIP6 ensemble	Coupled Model Intercomparison Project, Phase 6	Eyring et al. (2016); Abernathy et al. (2021)	<a href="https://console.cloud.google.com/storage/browser/cmip6">https://console.cloud.google.com/storage/browser/cmip6</a>

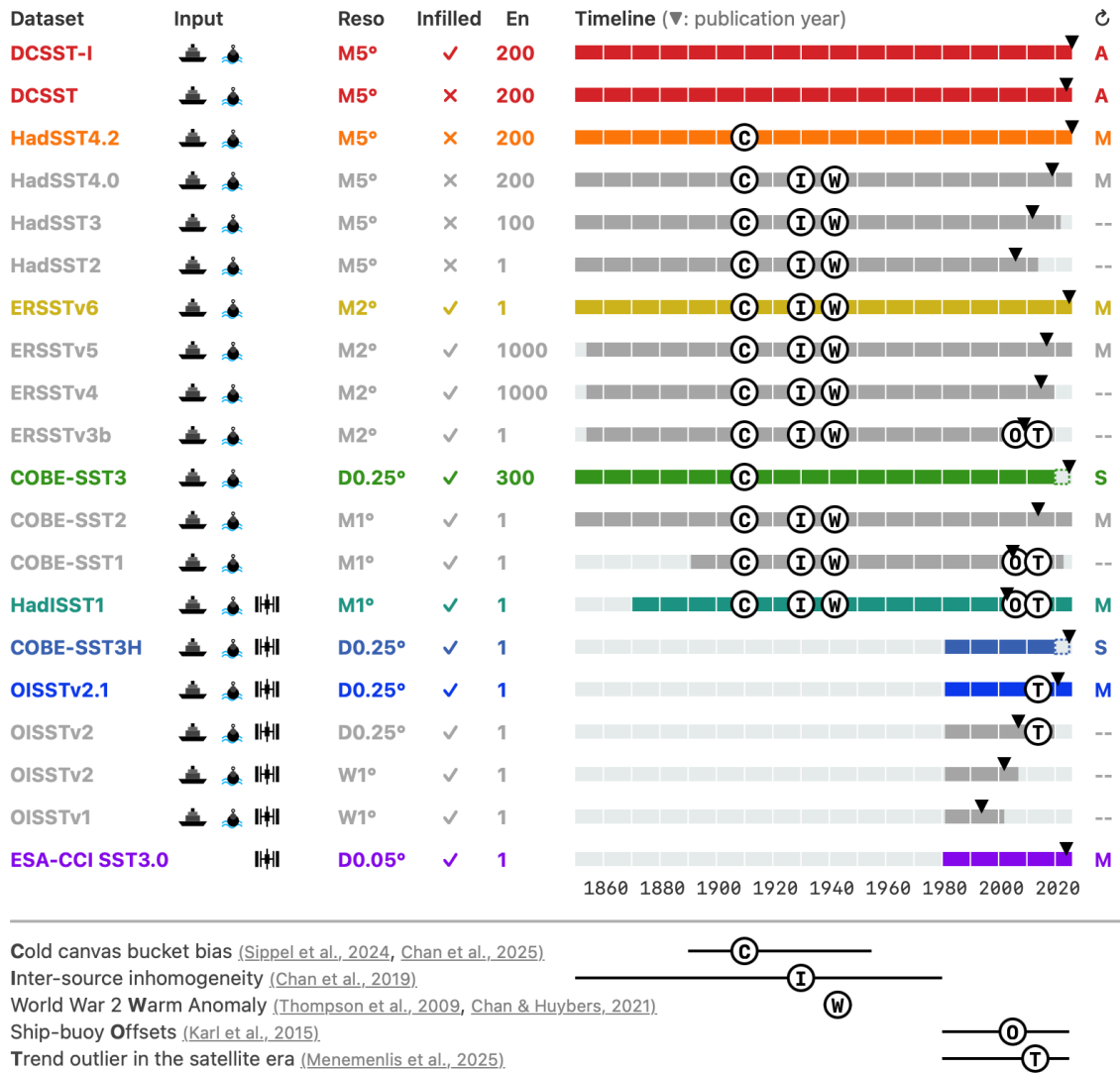


FIG. 1: Overview of major SST dataset families: DCSST (red); HadSST (orange); ERSST (yellow); COBE-SST (green); HadISST (teal); COBE-SSTH (light blue); OISST (blue) and ESA CCI SST (purple). Datasets are grouped by family and ordered by version within each family. Gray indicates non-current dataset versions within each family. Columns indicate input data types (Input: ship/ buoy/ satellite), nominal temporal (Monthly/ Weekly/ Daily) and spatial ( $^{\circ}$ ) resolution (Reso), spatial completeness (Infilled:  $\checkmark/\times$ ), ensemble size (En), temporal span (horizontal bar in Timeline), publication year (downward black triangle in Timeline), and update frequency ( $\cup$ : Annual/ Monthly/ Static/ Discontinued (- -)). Symbols mark major known biases and artifacts that remain in each product: cold canvas bucket bias (C), inter-source inhomogeneity (I), World War II warm anomaly (W), ship-buoy offsets (O), and trend outliers in the satellite era (T), based on evaluations presented in section 2 and 3. Indicative ranges for these issues are shown in the legend below. Dataset abbreviations follow those in the text and are expanded in Table 1

- 65 1. Long historical *in situ* records beginning before 1900, e.g. HadSST, ERSST and COBE-SST,  
 66 intended for decadal- to centennial-scale climate applications. These products often provide  
 67 the oceanic component for global surface temperature datasets and new major versions are

68 released approximately every six years aligned with the Intergovernmental Panel on Climate  
69 Change (IPCC) assessment cycle.

- 70 2. High-resolution SST analyses, e.g. ESA CCI SST and NOAA OISST, over the era of sustained  
71 satellite observations since 1980. These datasets utilize remotely sensed SST observations,  
72 may blend with *in situ* measurements, and provide data at high spatial and temporal resolutions.  
73 Several satellite-era analyses are also updated in near-real time for weather and climate  
74 prediction applications.
- 75 3. Centennial and multi-decadal records that combine long-term *in situ* observations with satellite  
76 data, where available, to achieve extended temporal coverage and greater spatial completeness  
77 whenever possible, often for use in atmospheric reanalyses or as boundary conditions for  
78 atmosphere-only dynamical models. An example is HadISST.

79 The creation of an SST product generally requires four elements: (1) data selection (and, in the  
80 case of satellite-based products, inference of SST from top-of-atmosphere measurements); (2) bias  
81 corrections to remove artifacts in measurements; (3) gridding and infilling to provide estimates  
82 in regions without direct measurements; and (4) derivation of an estimate of uncertainty for each  
83 value in the final product. Each element has improved over the years, leading to updated versions  
84 of the long-standing product families as well as newly-developed datasets, e.g. DCSST.

85 Despite these advances, uptake of newer SST datasets by the research community can be slow. As  
86 a result, some datasets that do not contain any bias adjustments, e.g., the gridded summaries from  
87 the International Comprehensive Ocean-Atmosphere Data Set (ICOADS, Freeman et al. 2017), or  
88 older products with outdated bias adjustments, e.g., the Kaplan SST (Kaplan et al. 1998), remain  
89 highly cited and widely used years after release, e.g., for long-term trends in the Tropical Pacific  
90 zonal SST gradient (Lee et al. 2022). Another example is HadISST1 (released 2003), which  
91 remains among the most cited SST datasets in 2025, but is one of few products not to correct  
92 for post-1950 ship-based SST biases. This bias leads to lower warming rate estimates since 2000  
93 (Karl et al. 2015) and thus systematically different estimates of recent trends (Menemenlis et al.  
94 2025). These are just a few of many examples of the mismatch between the SST products most  
95 widely used in research and those that best reflect current understanding of observational biases  
96 and uncertainties.

97 This lag in adoption reflects the reality of research where “switching costs” can be high. Fa-  
98 miliarity often shapes dataset choice, while barriers such as non-standard data formats, large data  
99 volumes, difficulty finding the data, and historically fragmented documentation create further fric-  
100 tion. The landscape has undoubtedly improved in recent years with comprehensive documentation  
101 now available in data journals (see Table 1) and user guides (e.g., HadSST4 and ESA CCI SST).  
102 Although fully absorbing the technical details of multiple candidate datasets may not seem an  
103 obvious priority, we show in this paper that where scientific analyses depend critically on observa-  
104 tional estimates of SST, selecting suitable products is essential for robust and high-quality research.  
105 Promoting these improved SST products is also timely as the climate community is determining  
106 standards for the upcoming IPCC CMIP7 and AR7, shaping the next years of climate science  
107 (Beadling et al. 2026).

108 This paper provides a starting point for SST users in navigating this evolving landscape, enabling  
109 them to more easily identify and consult relevant data papers and user guides for informed choices  
110 of SST products best suited for their particular application. Specifically, this paper addresses the  
111 questions: “Why do datasets differ?” by tracing the evolution of their development in section 2,  
112 “What do these differences mean for climate analyses?” by comparing products in section 3, and  
113 “How do I pick SST datasets?”, by providing guidance on the current state-of-the-art as well as  
114 anticipated improvements likely to affect future choices in section 4. Section 5 provides a summary.

115 Our analysis focuses on long-standing and recently developed SST dataset families that are  
116 updated regularly. We exclude older products whose methods have not been updated since before  
117 2000 (e.g., Kaplan SST) or that lack bias adjustments (e.g., gridded ICOADS), due to their limited  
118 comparability with modern products. Several high-quality near-real-time analyses are omitted  
119 because they are either shorter than forty years (e.g., the Multiscale Reanalysis by Chin et al.,  
120 2017 and the Canadian Meteorological Center analysis by Brasnett et al., 2018) or built on a  
121 significant input of ESA CCI SST data (e.g., the OSTIA reprocessing by Worsfold et al., 2024).  
122 Operational SST analyses that principally support numerical weather prediction are coordinated  
123 by the Group for High Resolution Sea Surface Temperature (GHRSSST, [www.ghrsst.org/](http://www.ghrsst.org/)), and  
124 inter-comparisons of these datasets have been reported elsewhere (e.g., Fiedler et al. 2019; Yang  
125 et al. 2021).

126 We also exclude hybrid datasets and reanalysis-derived SST fields. This includes blends of  
127 different products made for reanalysis (e.g. Hersbach et al. 2020) and surface-forcing datasets for  
128 AMIP-style uncoupled simulations that combine HadISST1 and OISSTv2 (Hurrell et al. 2008).  
129 Atmospheric reanalyses, such as ERA5, are driven by externally specified SST boundary conditions  
130 that often draw on products already discussed here, and therefore do not provide independent SST  
131 analyses. Ocean reanalyses and state estimates, such as GLORYS12V1 (Jean-Michel et al. 2021)  
132 and ECCO (Forget et al. 2015), produce essentially model-simulated SST fields that are continually  
133 corrected using multiple sources of observations, including satellite SST, subsurface temperature,  
134 sea level, sea ice, and salinity. These SST fields are therefore not derived from SST observations  
135 alone and are not directly comparable to the products reviewed here.

## 136 **2. History of SST Products and Recent Advances**

137 This section reviews how three core elements of SST product development – bias adjustment,  
138 gridding and infilling, and uncertainty quantification – have evolved, with each stage discussed in  
139 its own subsection.

### 140 *a. Bias adjustment*

141 Biases in SST records stem from pervasive and systematic errors that differ between measurement  
142 methods and platforms, their changing mix over time and their past data curation and processing  
143 (Kent and Kennedy 2021). Ship-based observations made with buckets are typically cold-biased  
144 because of evaporative cooling, and different bucket types used by various nations and periods left  
145 distinct bias signatures. On the other hand, engine-room intake (ERI) measurements tend to be  
146 warm-biased owing to heat from the vessel (Kent and Taylor 2006). These biases are often several  
147 tenths of a degree Celsius in magnitude and distort long-term trends, making their correction a  
148 central task in development of climate-quality analyses.

149 Early adjustment efforts concentrated on pre-1940 bucket biases. An initial blanket adjustment  
150 (Folland et al. 1984) was followed by land-anchored estimates using coastal station temperatures  
151 (Jones et al. 1986) and, soon after, physics-based bucket models that simulated cooling as a function  
152 of bucket type and usage (Bottomley et al. 1990; Folland and Parker 1995). Because detailed  
153 metadata on bucket types and national practices are sparse, these schemes necessarily assumed

154 simplified and broadly timed transitions, yielding limited regional differentiation, as implemented  
155 in, e.g., HadSST2. In parallel, ERSSTv3b pursued an anchoring strategy using nighttime marine  
156 air temperatures (Smith and Reynolds 2002; Kent et al. 2013), although adjustments were still only  
157 applied prior to 1940.

158 A major indication of biases present in engine-room-intake (ERI) temperatures, which caused  
159 a spurious decrease in global mean surface temperature by approximately 0.3°C following World  
160 War II, was discovered by Thompson et al. (2008). ERI measurements represent the majority of  
161 SST data available between 1930 and 1990 (Kent and Taylor 2006). Subsequent datasets (e.g.,  
162 HadSST3 and COBE-SST2) extended bias corrections beyond 1940 to account for ERI biases as  
163 well as offsets between ship-based and buoy measurements. Time-varying offsets between ship-  
164 based and buoy measurements shown to affect post-2000 temperature trends (Karl et al. 2015) were  
165 accounted for starting ERSSTv4, HadSST4.0 and COBE-SST2.

166 Since 2019, attention has expanded from method-specific biases to finer spatial and platform-  
167 dependent structures. HadSST4.0 used near surface values from marine profile temperatures to  
168 estimate regional, ship-related biases after 1940. In parallel, Chan and Huybers (2019) developed  
169 an intercomparison framework that quantifies offsets among national groupings and enables pre-  
170 1940 comparisons. This framework has revealed a cold truncation bias in part of the Japanese  
171 data that contributed to the unusually heterogeneous early-20<sup>th</sup>-century warming pattern (Chan  
172 et al. 2019). This truncation bias has recently been adjusted in DCSST(-I), COBE-SST3, and  
173 HadSST4.2 through different implementations.

174 The most recent identification of *in situ* bias is a global cold bias in decades around the 1910s  
175 (Chan et al. 2023; Sippel et al. 2024) that alters estimates of early warming and decadal variability  
176 and is attributed to incomplete correction of canvas bucket temperatures (Chan et al. 2025). To  
177 date, only DCSST and COBE-SST3 implement specific adjustments to account for this global cold  
178 bias by reviving the earlier land-anchoring idea (Jones et al. 1986).

179 Satellite SSTs are obtained from relatively few (~25) missions with differing bias characteristics  
180 (e.g. Yang et al. 2021; Fiedler et al. 2019). These platform-dependent effects are also on the order  
181 of several tenths of a degree Celsius (Merchant et al. 2008b). Satellite SST records have further  
182 required corrections for biases from atypical atmospheric conditions, particularly the stratospheric  
183 aerosol from the 1991 Pinatubo eruption (Reynolds 1993; Merchant et al. 1999).

184 The satellite-only ESA CCI SST is based on physics-based estimation approaches (Merchant et al.  
185 2008a; Embury and Merchant 2012; Merchant et al. 2020a) to minimize biases from changing  
186 satellite characteristics and from volcanic perturbations to the stratosphere. The local time of  
187 satellite overpasses has varied, and the artificial trends arising from changing observation times  
188 relative to the daily cycle of SST are also addressed in ESA CCI SST through adjustments to a  
189 standard local time of observation. ESA CCI SST also explicitly adjusts the skin temperature  
190 observable from space to estimate the SST at 20 cm depth for compatibility with centennial-scale  
191 datasets using *in situ* data from drifting buoys and buckets.

192 To sum up, both *in situ* and satellite SST measurements are affected by systematic biases, and  
193 recognizing these biases and developing adjustments has taken time. The development of SST  
194 analyses has therefore progressed from broad, method-based corrections toward more spatially ex-  
195 plicit and platform-specific treatments. This history of improved understanding of the observations  
196 over time, alongside advances in numerical techniques and computing capacity, is one key reason  
197 why SST products differ.

#### 198 *b. Construction of gridded fields*

199 Typically, individual observations are first assigned to the appropriate grid cell and temporal  
200 window (e.g., month/day) and averaged to estimate the mean SST within each cell-window combi-  
201 nation. An obvious difference between products is therefore the spatial and temporal grid resolution  
202 (here ranging from 5° monthly to 0.05° daily; Fig. 1). This choice is largely shaped by application  
203 needs tempered by data and processing limitations. For example, while monthly 5 or 2° products  
204 (such as HadSST and ERSST products) are usually sufficient for studying slowly varying climate  
205 backgrounds and large-scale modes of variability, much higher spatial and temporal resolution,  
206 such as is available from satellite-based records, is required for resolving extreme events like marine  
207 heat waves. Within a family, some products have trended toward finer resolution, as in OISST  
208 and COBE-SST (Fig. 1). For example, compared with its predecessor, COBE-SST3 provides a  
209 finer daily 0.25° resolution, designed to better capture mesoscale variations and steep meridional  
210 gradients that are important for understanding fine-scale air–sea interactions relevant to significant  
211 weather events.

212 A relevant concept is the distinction between nominal grid resolution and effective resolution  
213 (Reynolds et al. 2013). In other words, a finer grid does not guarantee that smaller-scale physical  
214 variations are always resolved. This distinction is particularly important for products that blend  
215 *in situ* and satellite data while aiming to provide a consistent nominal resolution across more  
216 than a century. HadISST1, for instance, has an effective resolution of about 4° before 1949,  
217 reflecting the reduced-space reconstruction used at that time (Rayner et al. 2003). Some products  
218 address this issue by offering separate versions, such as COBE-SST3, which extends back to 1850  
219 without satellite data, and COBE-SST3H, which incorporates satellite measurements but only  
220 from 1982 onward (Fig. 1). Thus, fine-scale variability in COBE-SST3 before the satellite era,  
221 and especially before the widespread deployment of drifting buoys, can only be reliably estimated  
222 in areas neighboring observations; estimates elsewhere should be treated as useful probabilistic  
223 reconstructions. Users interested in fronts, coastal upwelling, western boundary currents, or other  
224 sharp gradients should therefore consider not only the nominal grid spacing, but also the period,  
225 sampling coverage, and effective resolution of each product.

226 After gridding data, a further application-oriented difference is how regions and times with  
227 no observations are handled. Non-infilled datasets such as the HadSST family leave those grid  
228 cells as missing and are often preferred for climate monitoring as they are closer to the original  
229 observations. In contrast, infilled products have values for those cells inferred using a variety of  
230 statistical methods and are generally more convenient to use, but their traceability to the original  
231 observations is weakened because spatial completeness is achieved by making assumptions about  
232 the variability.

233 Infilling methods typically define the expected relationship between conditions at different loca-  
234 tions using a covariance matrix. The simplest choice of covariance between locations is isotropic  
235 and homogeneous, but more complex empirical relationships can be assumed to better capture  
236 regional variations in covariance, as implemented in DCSST-I and high-resolution satellite-based  
237 products such as ESA CCI SST and COBE-SST3H. Other methods explicitly account for long-  
238 range teleconnections, including Reduced-Space Optimal Interpolation (Kaplan et al. 1997, e.g.,  
239 in HadISST1), reconstructions based on Empirical Orthogonal Functions (EOFs, Hirahara et al.  
240 2014, e.g., in COBE-SST2 and 3), and Empirical Orthogonal Teleconnections (EOTs, Smith et al.  
241 1998, e.g., in ERSSTv3–v5).

242 Improvements in infilling across products in the same family can also be evident. For example, an  
243 increasing number of EOT modes have been used in successive ERSST versions to better capture  
244 localized variability. In its latest version (ERSSTv6), a three-layer fully connected neural network  
245 is used to replace EOT and has yielded better infilling skill (Huang et al. 2025).

### 246 *c. Uncertainty estimation*

247 Quantifying uncertainty is essential for making appropriate use of SST datasets (Kennedy 2014).  
248 Most products provide uncertainty values per grid box and/or time step (e.g., ESA CCI SST, COBE-  
249 SST1–2), ensembles of plausible realizations (e.g., ERSSTv4–v5, DCSST(-I), COBE-SST3), or  
250 both (e.g., HadSST3–4.2), for uncertainty quantification. Some older products (such as HadISST1)  
251 do not provide uncertainty estimates.

252 Ensembles are convenient for tracing how uncertainty propagates into climate analyses: a diag-  
253 nostic is repeated for each member and the across-member distribution defines confidence intervals  
254 consistent with observational error covariance. Ensembles can quantify complex error structures  
255 which cannot be handled analytically. Because individual members may contain more small-scale  
256 variability than the ensemble mean or median, variance statistics based on individual members can  
257 differ from those on the central measure alone. Moreover, for a given product, the across-member  
258 spread reflects only the uncertainty associated with choices internal to that product’s particular  
259 methodology (known as “parametric uncertainty”).

260 A more complete accounting of uncertainty must also reflect the full range of methodological  
261 choices in input data, quality control, bias adjustment, and reconstruction. This “structural un-  
262 certainty” is commonly approximated by the spread across independently developed SST datasets  
263 (Thorne et al. 2005), assuming they are diverse enough to span the plausible error range. How-  
264 ever, many products share observational archives and methodological lineages, leading to common  
265 issues. For example, the SST datasets used in the last IPCC assessment all exhibited an early-20<sup>th</sup>-  
266 century cold anomaly (Sippel et al. 2024, represented here as the cold canvas bucket bias in Fig. 1),  
267 despite their apparent diversity. This cautions data users against treating inter-product agreement  
268 as evidence that structural uncertainty has been fully explored, and highlights the need for genuine  
269 diversity in reconstruction approaches across the entire dataset development cycle.

270 These advances in bias adjustment and the construction of gridded fields, along with the addition  
271 of newly-available historical data, provide SST products that better represent the historical evolution  
272 of SST than their predecessors, as illustrated in the next section.

### 273 **3. Comparison of Products**

274 This section evaluates and compares SST datasets across a range of metrics to help data users  
275 determine which products reliably represent the phenomena and scales of variability relevant to  
276 their applications. Specifically, we investigate to what extent SST products exhibit bias signatures  
277 associated with known data artifacts (Section 3a, Figure 2); the spatial structures of events such  
278 as ENSO and marine heatwaves (Section 3b, Figure 3); and climate features including long-term  
279 warming, major modes of variability, and important regional gradients (Section 3c, Figure 4).

#### 280 *a. Bias signatures*

281 Fig. 2a shows global-mean annual SST anomalies from each of the data products since 1850.  
282 The focus in this section is the pre-1960 evolution, because this is where differences between SST  
283 products are most pronounced due to remaining data biases.

284 State-of-the-art CMIP6 simulations are shown for context. Compared with observational prod-  
285 ucts, the CMIP6 ensemble mean shows a much smoother evolution of global-mean SST because  
286 averaging across many simulations largely cancels internally generated variability, such as ENSO,  
287 leaving primarily the response to external forcing. Differences between the CMIP6 ensemble  
288 and the observations, however, do not arise from internal variability alone, but may also reflect  
289 biases in the models, their forcings, or the observational products (Chan 2021). In most contexts,  
290 such discrepancies are used to assess model performance. However, if observational biases are  
291 not independently identified and accounted for (through careful analysis of the constituent data  
292 sources supported by documentary evidence indicating changes in observing protocols or data  
293 management), model–data discrepancies may be misattributed to the models or lack of physical  
294 understanding, leading to misleading evaluations. We illustrate this below using three examples.

295 The first is the World War II warm anomaly (Fig. 2b; Table 2), which is due to wartime changes  
296 in measurement practice that introduced warm biases (Thompson et al. 2008; Chan and Huybers  
297 2021). Accounting for these issues, COBE-SST3, HadSST4.2, and the new DCSST family all

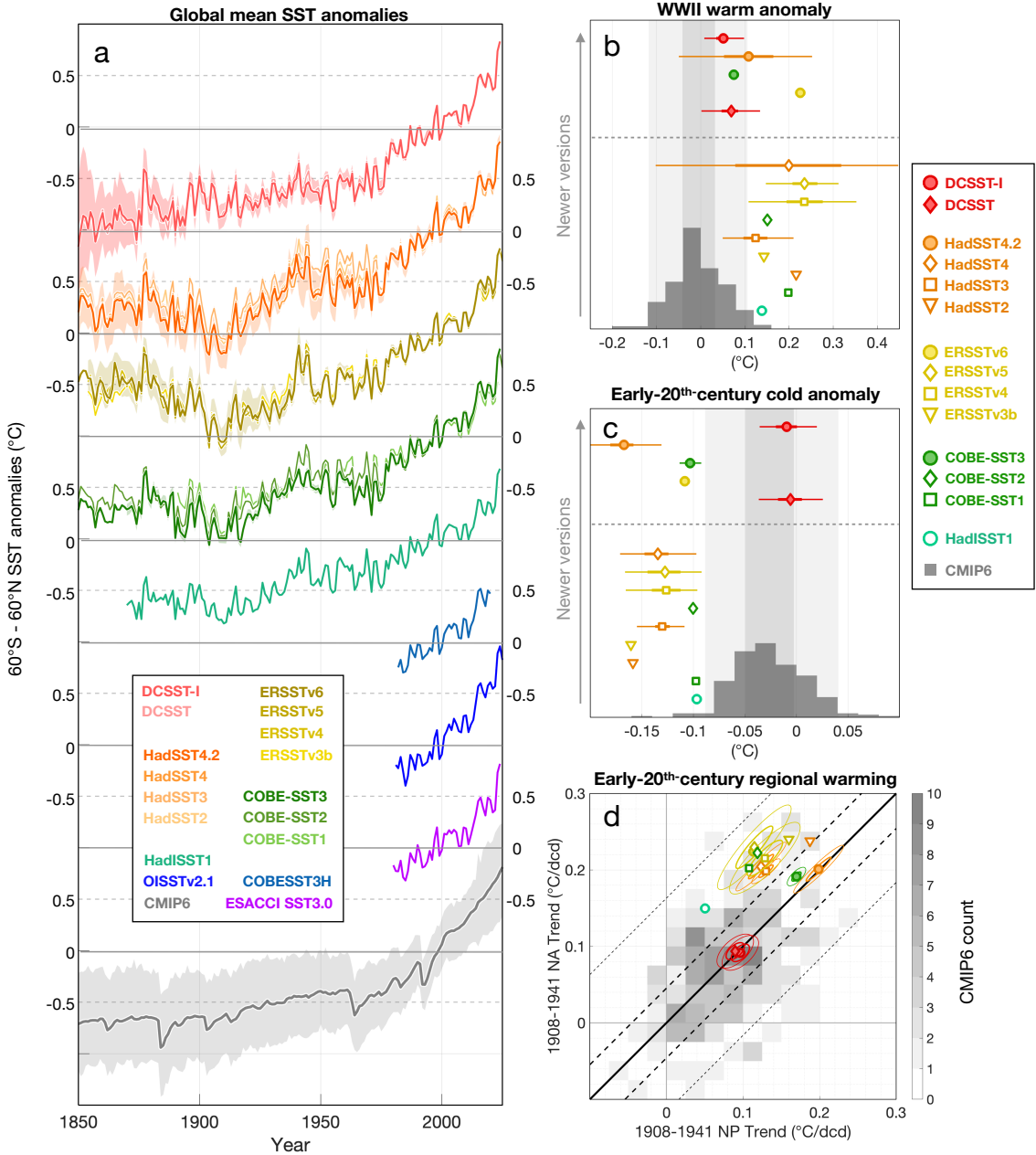


FIG. 2: **Comparison of global mean SST and data artifacts.** (a) global mean SST anomalies relative to 1982–2014 climatology. Datasets are grouped and offset by families. Here, “global” is defined as 60°S–60°N to focus on the ice-free ocean, where SST is more consistently defined and comparable across products. Also, only 10% of the global ocean surface is poleward of 60°N/S. Within each family, thick color-coded lines show central estimates for individual versions, and the shading shows the 95% c.i. for the latest release where an ensemble is available. Simulations from 229 CMIP6 runs, concatenating historical and SSP2-4.5 experiments, are shown at the bottom. (b) World War II warm anomaly, calculated as the global mean SST anomaly over 1941–1945, relative to the mean over 1936–1940 and 1946–1950. Markers, sorted by publication dates (descending) in the y-axis, denote the mean value of a dataset, while thick and thin lines, respectively, denote the interquartile range and 95% confidence interval (c.i.), where an ensemble is available. The dashed line separates state-of-the-art and older products. The histogram presents the CMIP6 distribution, and the dark and light shading denotes, respectively, the interquartile and 95% c.i. (c) as (b) but for early-20<sup>th</sup>-century cold anomaly, defined as the global mean SST over 1900–1930 minus a reference given by a linear trend fitted to the periods 1890–1899 and 1931–1940. (d) North Atlantic (y-axis) versus North Pacific (x-axis) SST trends over 1908–1941. Markers are as (b), and ellipses denote 1 s.d. and 2 s.d. uncertainty using a bi-variate Gaussian fit. The heat map squares represent the 2D histogram of CMIP6 historical simulations and the black line depicts the one-to-one relationship, and thick and thin dashed lines denote, respectively, the interquartile range and 95% c.i. of the simulated inter-basin trend difference. Note that CMIP6 values plotted are based on global coverage for 60°S–60°N so do not match coverage for the HadSST family.

TABLE 2: Definitions and calculation methods for metrics used in this study.

Metric Name		How to calculate?
Global SST		Area-weighted (cosine latitude) mean over 60°S–60°N oceans, following Menemenlis et al. (2025).
Early-20 <sup>th</sup> -Century Anomaly	Cold	Global mean SST difference over 1900–1930 relative to a linear fit between 1890–1899 and 1931–1940, following Sippel et al. (2024).
WWII Warm Anomaly		Global mean SST anomaly averaged over 1941–1945 relative to the mean of 1936–1940 and 1946–1950, following Chan and Huybers (2021)
North Pacific SST		Area-weighted mean over 20°N–60°N, 100°E–100°W, following Chan et al. (2019).
North Atlantic SST		Area-weighted mean over 20°N–60°N, 100°W–10°E (excluding Mediterranean), following Chan et al. (2019).
Early-20 <sup>th</sup> -Century Warming	Warming	Linear trend of global mean SST over 1908–1941, following Chan et al. (2019).
Warming Level since the Pre-industrial Baseline		Difference in global-mean SST over 2014–2023 relative to 1850–1900.
Niño3.4 SST		Area-weighted mean over 5°S–5°N, 170°W–120°W, following Trenberth (1997).
West Equatorial Pacific SST		Area-weighted mean over 5°S–5°N, 110°E–180°, following Watanabe et al. (2021).
East Equatorial Pacific SST		Area-weighted mean over 5°S–5°N, 180°–80°W, following Watanabe et al. (2021).
Southern Ocean		Area-weighted mean over 50°S–70°S, following Dong et al. (2023).
AMV Index		The difference between 20-year running smoothed monthly North Atlantic SST anomalies (0°–60°N, 80°W–0°E) and global SST, following Trenberth and Shea (2006).

298 show smaller warm anomalies than older products. This reduced warm anomaly is consistent  
 299 with independent evidence from coral proxies (Pfeiffer et al. 2017) and with a large El Niño event  
 300 identified in upper-air measurements spanning 1939–42 (Brönnimann et al. 2004). Correcting data,  
 301 therefore, changes the interpretation of model–data differences during this period, which might  
 302 otherwise be interpreted, for example, as indications of deficiencies in the prescribed external  
 303 forcings (Gottschalk 2017). ERSST is now the only major product family in which a pronounced  
 304 World War II warm anomaly persists.

305 Another example is the early 20th century cold anomaly (Fig. 2c), during which older and some  
 306 state-of-the-art products show pronounced negative anomalies. HadSST4.2 appears particularly  
 307 cold because the truncation bias adjustment applied in the 1930s increases SST in the reference  
 308 period used here (Table 2). As described in Section 2a, the cold anomaly likely reflects a residual  
 309 bias arising from incomplete correction of canvas bucket measurements (Sippel et al. 2024).  
 310 DCSST uses an adjustment anchored to land temperatures (Chan et al. 2024b) and shows SST  
 311 evolution more consistent with collocated coral proxies (Chan et al. 2025). DCSST and DCSST-I

312 accordingly show the smallest cold anomaly, reflecting a more moderate but consistent warming  
313 from 1850 to 1940. This suggests that the model-data mismatch in earlier attribution studies of  
314 this period, in which climate models could explain only about half of the observed temperature  
315 trend (Hegerl et al. 2018), may partly reflect residual bias in the SST products used rather than  
316 deficiencies in the models or prescribed forcings alone.

317 On regional scales, correcting the Japanese truncation bias directly alters the contrast in early-  
318 20<sup>th</sup>-century warming between the North Pacific and North Atlantic (Chan et al. 2019). For older  
319 products, all families show the North Atlantic warming nearly twice as fast as the North Pacific over  
320 1908–1941 (Fig. 2d), a contrast that could only be explained by an unusually large expression of  
321 internal variability (Delworth and Knutson 2000). In the latest versions, HadSST4.2, COBE-SST3,  
322 and DCSST correct for this bias, bringing the inter-basin warming rates much closer to each other.  
323 ERSSTv6, by contrast, still exhibits a pronounced inter-basin difference, similar to earlier ERSST  
324 releases. Data bias may, therefore, have contributed to the previously inferred inter-basin contrast,  
325 with implications for assessment of internal variability in models.

326 Overall, the incorporation of adjustments for newly identified artifacts into SST data production  
327 has been gradual. Nevertheless, recent products generally account for a wider range of known  
328 biases and are more internally consistent than earlier versions. This evolution also highlights that  
329 when models and data disagree, discrepancies cannot be assumed to arise solely from models  
330 or prescribed forcings. More broadly, observational products, especially century-long historical  
331 products, should not be treated as fixed benchmarks against which successive generations of climate  
332 models are evaluated. Using SST products with more complete bias corrections can materially  
333 alter the interpretation of model–data differences and the evaluation of model performance.

### 334 *b. Gridding and Infilling*

335 The different choices in the reconstruction of gridded products, including resolution and infilling,  
336 are important to consider for some applications. When studying historical events with sparse  
337 observations, spatial infilling and smoothing can make analyses more convenient, but the resulting  
338 fields are highly dependent on the assumptions used to generate complete fields. Taking the 1877  
339 El Niño as an example, only a few ship tracks crossing the equator exist in the Pacific basin as shown  
340 in the non-infilled product HadSST4.2 (Fig. 3a<sub>1</sub>). Infilled products using isotropic, homogeneous

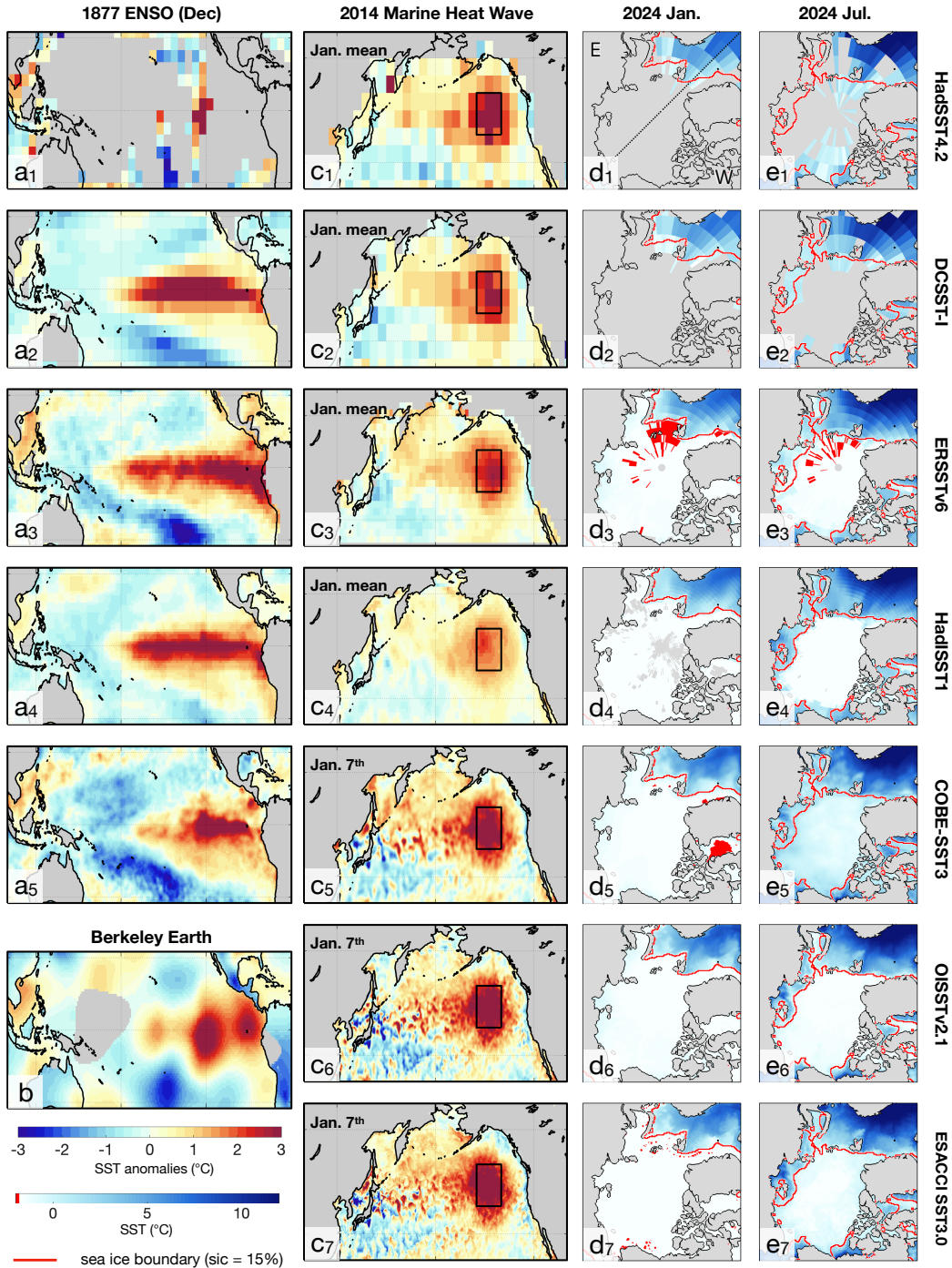


FIG. 3: **Comparison of spatial patterns.** Column (a) shows December 1877 SST anomalies relative to the 1982–2014 December climatology. Rows (top to bottom) show HadSST4.2, DCSST-I, ERSSTv6, HadISST1, and COBE-SST3. (b) as (a) but for the Berkeley Earth surface temperature. Column (c) shows January 2014 SST anomalies relative to the January climatology over the same period, highlighting the marine heatwave termed “the Blob” in the North Pacific for datasets as in (a) but also including OISST and ESA CCI SSTv3. For datasets with daily resolution (COBE-SST3, OISSTv2.1, and ESA CCI SSTv3), the maps correspond to January 7, 2014, when the event peaked. The black box (140–155°W, 38–50°N) marks the region used to calculate the intensity of this event. Columns (d) and (e) show actual SSTs over the Arctic in January and July 2024, respectively. Red curves mark the sea-ice edge ( $\geq 15\%$  sea-ice concentration, Cavalieri et al. 2011), gray areas indicate missing values, and red regions denote SSTs below the  $-1.8^{\circ}\text{C}$  freezing point. In panel d<sub>1</sub>, the diagonal dashed line marks the  $0^{\circ}$  and  $180^{\circ}$  meridians with Eastern (E) and Western (W) Hemispheres labeled.

341 covariance structures, e.g., Berkeley Earth surface temperature <sup>1</sup> (Rohde and Hausfather 2020),  
342 produce patterns consistent with their round kernels (Fig. 3b). By contrast, more advanced  
343 approaches, including anisotropic kernels (DCSST-I, Fig. 3a<sub>2</sub>), AI-based methods (ERSSTv6,  
344 Fig. 3a<sub>3</sub>), and EOF-based reconstructions (HadISST1, Fig. 3a<sub>4</sub>; COBE-SST3, Fig. 3a<sub>5</sub>), yield  
345 more coherent El Niño structures resembling the canonical pattern seen in the satellite era. Fine-  
346 scaled structure still differs between products as the fields are only tightly constrained by nearby  
347 observations. For example, the positive anomaly extends further west in DCSST-I and ERSSTv6  
348 than in COBE-SST3, contributing to the structural uncertainty across the datasets.

349 For contemporary extreme events such as marine heatwaves, data availability is not the limiting  
350 factor. Rather, the requirement is to resolve fine spatial and temporal scales. Taking the North  
351 Pacific “Blob” of January 2014 as an example, all products — including the non-infilled monthly  
352 5° HadSST4.2 — show a similar warm anomaly centered near 145°W, 45°N (Fig. 3c). However,  
353 monthly fields blur the peak intensity evident in daily analyses. Over a box spanning 140–155°W,  
354 38–50°N (black box in Fig. 3c), the mean SST anomaly in January is 2.5°C in DCSST-I, 2.4°C  
355 in ERSSTv6, 2.9°C in HadSST4.2, and only 1.7°C in HadISST1, whereas on the peak date  
356 (January 7) in daily products the corresponding values are higher (3.0°C for COBE-SST3, and  
357 3.1°C for OISSTv2.1 and ESA CCI SST). The daily high-resolution fields in Fig. 3 also reveal  
358 eddy-scale variability and fine filaments, which may be important for understanding the evolution  
359 and mechanisms of marine heatwaves and their ecosystem impacts (Bian et al. 2023).

360 Another example of reconstruction differences arises in polar regions, where the open ocean  
361 meets sea ice. Due to sparse *in situ* coverage in polar regions, some products (e.g., DCSST-I) omit  
362 SST values in grid cells with no open ocean values (Chan et al. 2026). Others, such as the COBE-  
363 SST family, use observationally-derived sea-ice concentration (SIC) with an empirical SIC–SST  
364 relationship that anchors SST to a spatially varying freezing point under high SIC (Hirahara et al.  
365 2014). Satellite products such as OISST (Huang et al. 2021) and ESA CCI SST (Embury et al.  
366 2024) adopt similar concepts, using product-specific freezing-point constraints in ice-covered grid  
367 cells.

368 Fig. 3d compares absolute Arctic SSTs in January 2024. Infilled products broadly follow  
369 the observed ice edge, though ERSSTv6 and COBE-SST3 exhibit below freezing point temper-

---

<sup>1</sup>Note that the Berkeley product SST is an infilled version of HadSST4.0 and is shown here to illustrate this effect. As a combined land–sea dataset, it is not used elsewhere in this SST-focused review.

370 atures within ice-covered regions. Such behavior may not matter for climate analyses where  
371 sea-ice-covered regions are masked. However, in AMIP simulations, the atmospheric model  
372 sees a weighted average of water and sea ice boundary conditions within each atmospheric grid  
373 cell. Hence, physically incompatible SST and SIC fields should be used with caution for such  
374 applications. Arctic summertime SST estimates in July 2024 diverge even more (Fig. 3e) in both  
375 open-ocean regions such as the Laptev–East Siberian Sea (at left of panels) and areas with partial  
376 ice cover, indicating that model runs using summertime boundary conditions could be especially  
377 sensitive to dataset choice in sea-ice-affected regions.

### 378 *c. Climate indicators of variability and change*

379 Beyond grid-level maps, widely used climate indicators such as global warming levels, regional  
380 trends, and metrics of climate variability, could depend strongly on the choice of SST products.  
381 Here, we examine several such indicators to demonstrate this sensitivity.

382 Estimates of long-term warming in global mean SST (60°S–60°N) remain sensitive to product-  
383 specific treatments of nineteenth- and early-20<sup>th</sup>-century biases (Fig. 4a, sections 2a and 3a), with  
384 newer products only slightly narrowing the range. Here, we quantify warming using the 2014–2023  
385 mean relative to 1850–1900 because this directly measures the present-day state relative to the IPCC  
386 pre-industrial baseline, while avoiding the assumption that warming evolves linearly over the full  
387 record. On this basis, excluding older datasets narrows the estimated SST warming range from  
388 0.7–1.0 to 0.8–1.0°C. This qualitative conclusion is unchanged when warming is instead quantified  
389 using the 1870–2023 trend (Fig. S1a), 2019–2023 mean relative to 1850–1900 baseline (Fig. S1b),  
390 or trends computed from varying start years (Fig. S1c). There is also evidence that the ERSST  
391 family, which features pronounced cooling over 1850–1910 (Fig. 2a), is likely too warm in the late  
392 nineteenth century (Sippel et al. 2024; Chan et al. 2025), leaving scope for further narrowing of  
393 the observational range.

394 During the well-sampled satellite era, observational products are expected to agree more closely.  
395 Yet, when comparing older and modern datasets, Menemenlis et al. (2025) found a wide spread in  
396 the warming trend over the satellite era, reproduced here (Fig. 4b). Restricting this comparison to  
397 state-of-the-art products tightens the range among central estimates from 0.10–0.18 to 0.13–0.18°C  
398 per decade. This narrowing is qualitatively robust to the choice of trend window, as shown by

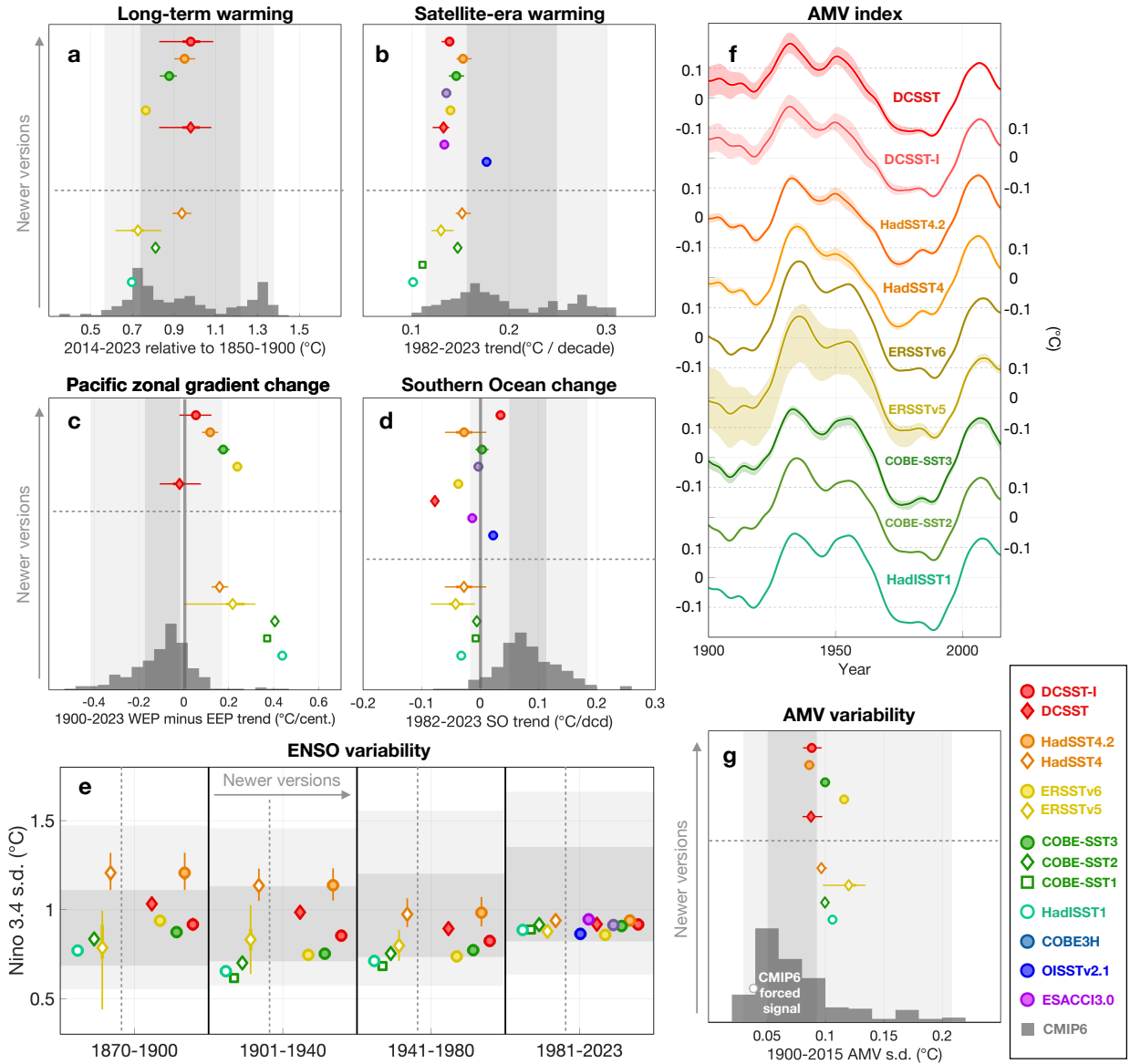


**FIG. 4: Comparison of key climate indices.** (a) Mean SST ( $60^{\circ}\text{S}$ – $60^{\circ}\text{N}$ ) for 2014–2023 relative to the 1850–1900 baseline, following the IPCC convention (Allan et al. 2023). Layout follows Fig. 2b and the dashed lines separate the older products from the most recent versions. Only products extending to 2023 are included. Error bars are shown where visible; in some cases they are smaller than the symbol size. (b) As in (a), but 1982–2023 linear trend; satellite products are also shown. (c) As in (a), but showing the 1900–2023 linear trend in Tropical Pacific zonal temperature gradient, defined as the difference between the west ( $5^{\circ}\text{S}$ – $5^{\circ}\text{N}$ ,  $110^{\circ}\text{E}$ – $180^{\circ}$ ) and the east ( $5^{\circ}\text{S}$ – $5^{\circ}\text{N}$ ,  $180^{\circ}$ – $80^{\circ}\text{W}$ ; Table 2). All products covering 1900 to 2023 are shown; the zero line is also highlighted. (d) As in (c), but for the 1982–2023 linear trend of SSTs over the Southern Ocean ( $50^{\circ}\text{S}$ – $70^{\circ}\text{S}$ ). (e) Standard deviation of monthly mean SST anomalies in the Niño 3.4 region ( $5^{\circ}\text{S}$ – $5^{\circ}\text{N}$ ,  $170^{\circ}\text{W}$ – $120^{\circ}\text{W}$ ), computed after removing the seasonal cycle and linear trend, for four periods: 1870–1900, 1901–1940, 1941–1980, and 1981–2023. Products are sorted by publication year in the direction indicated by gray arrows. Dark and light shading show the interquartile and 95% confidence intervals across CMIP6 simulations. (f) Twenty-year smoothed monthly AMV index for recently-updated century-long products. Series are vertically offset for clarity. (g) Standard deviation of the smoothed AMV index in (f). The white dot marks the s.d. of the multi-model mean, indicating the amplitude of the forced signal.

399 sensitivity tests varying the start year (Fig. S1c). Within this group, DCSST, ERSSTv6, COBE-  
400 SST3, and ESA CCI SST cluster near  $0.14^{\circ}\text{C}$  per decade, with HadSST4.2 being slightly higher at  
401  $0.15^{\circ}\text{C}$  per decade. NOAA's daily OISSTv2.1 is the clear remaining outlier ( $0.18^{\circ}\text{C}$  per decade),  
402 perhaps due to its fixed  $0.14^{\circ}\text{C}$  ship-to-buoy correction from 1981–2015. Hence, the observational  
403 spread in satellite-era SST warming is narrower than previous comparisons that included older  
404 datasets.

405 On regional scales, an important indicator is the Equatorial Pacific zonal SST gradient, which  
406 influences circulation, clouds, albedo, and climate sensitivity (Kang et al. 2023). Older products  
407 such as HadISST1 and COBE-SST1 show a pronounced century-scale strengthening of the zonal  
408 SST gradient (Deser et al. 2010), whereas this trend is substantially weaker in newer products, a  
409 result that is qualitatively unchanged when the trend start year is varied (Fig. 4c; Fig. S2a,c). This  
410 weakened enhancement in zonal SST gradient is more consistent with independent data including  
411 the sea-level pressure gradient and precipitation trend pattern (Deser et al. 2010). This result in  
412 turn weakens the case for a pronounced model–data discrepancy in zonal-gradient trends (Byrne  
413 et al. 2025). Note that it does not imply agreement across all trend windows (Fig. S2b,c), nor does  
414 it establish model fidelity. For example, mean-state biases, especially an overly cold equatorial cold  
415 tongue, in CMIP6 models can induce excessive eastern-Pacific warming and hence an erroneous  
416 weakening of the zonal SST gradient (Seager et al. 2019). Nevertheless, these results show that  
417 conclusions about model–data agreement are sensitive to the choice of SST products. Moreover,  
418 although newer products suggest a smaller long-term trend in the west–east gradient, the spatial  
419 pattern of SST trends still differs across products (Fig. S3), underscoring the need to further  
420 understand how bias adjustments and infilling choices affect observational estimates.

421 Southern Ocean SST is another key regional indicator, relevant to Antarctic sea-ice melt (Dong  
422 et al. 2022), heat uptake (Gregory et al. 2024), and the impact of Antarctic stratospheric ozone  
423 depletion (Schneider et al. 2015; Seviour et al. 2019). CMIP6 models generally suggest warming  
424 ( $-0.02$  to  $0.18^{\circ}\text{C}$  per decade) over 1982–2023, but observational products show trends closer to  
425 zero, with considerable spread (Fig. 4d). Spatial patterns also differ across products, particularly  
426 in the magnitude and extent of the cooling band (Fig. S4). Given the sparse *in situ* sampling in this  
427 region, satellite-based products are likely the most reliable for recent Southern Ocean assessments,  
428 which further suggests that models may be warming too strongly in recent years.

429 It is also informative to consider modes of climate variability, particularly ENSO. During the  
430 satellite era, observational products consistently show Niño-3.4 variability of 0.85–0.95°C (1 s.d.;  
431 Fig. 4e). Earlier in the record, however, observational estimates diverge. This divergence could  
432 arise from increased sampling and measurement uncertainty, as well as structural differences in  
433 interpolation methods. Combined with the intrinsic difficulty of estimating ENSO variance reliably  
434 from 30–50-year windows (Wittenberg 2009; Deser et al. 2012), these factors suggest that current  
435 SST datasets are unlikely to provide a reliable estimate of long-term changes in ENSO variability,  
436 even though CMIP6 models on average suggest an increase over time (Fig. 4e).

437 Finally, decadal modes of variability such as Atlantic Multidecadal Variability show broad  
438 consistency in phase among products (Fig. 4f), but differ slightly in amplitude (Fig. 4g). These  
439 amplitude differences are mainly family-specific and vary little across versions within a family.  
440 Compared with CMIP6 models, observational amplitudes tend to lie toward the higher end of the  
441 model spread, though they remain within the range sampled by individual simulation members.

442 Overall, state-of-the-art SST datasets now show better agreement with each other than their  
443 predecessors across a range of metrics. Differences are larger in long-term trends and in data-  
444 sparse regions, but they generally agree on global warming levels and major variability modes over  
445 the satellite era. For climate model evaluation, some model-observation discrepancies reported  
446 in the literature were amplified by biases in older SST products and are less pronounced when  
447 assessed using current datasets. Together, these results underscore the importance of being aware  
448 of how SST datasets have evolved and adopting up-to-date, well-documented releases matched to  
449 the intended analysis.

## 450 **4. How to Choose**

### 451 *a. Principles underpinning dataset choice and usage*

452 We have shown that careful dataset choice is crucial for high quality and robust analyses. With  
453 that in mind, there are practical considerations that may restrict dataset choice. These include  
454 the length of record, whether fields are spatially complete, spatial and temporal resolution, the  
455 availability and type of uncertainty estimates, and the immediacy of updates to include the most  
456 recent data. All datasets are free to use for research, but some have restrictions for other purposes  
457 such as commercial use that need to be checked and adhered to. The [web-based selector tool](#)

458 (similar to Figure 1) enables users to quickly view, subset, and access candidate datasets suitable  
459 for specific applications. When several products exist, results will be more robust if all are used.  
460 Typical dataset choices by application include:

- 461 • **Climate monitoring:** compare non-infilled and infilled datasets at monthly or higher resolu-  
462 tion.
- 463 • **AMIP forcing:** use infilled datasets at monthly or higher resolution.
- 464 • **Attribution or model–data comparisons:** use ensemble datasets (either infilled or non-  
465 infilled) with uncertainty estimates. For non-infilled products, apply the same observational  
466 coverage mask to the model output to ensure a fair comparison.
- 467 • **Western boundary currents, mesoscale eddy signatures, marine heatwaves:** use infilled  
468 high-resolution datasets (daily, finer than  $1^\circ \times 1^\circ$ ).
- 469 • **Paleo proxy calibration:** use long instrumental records without known issues during the  
470 calibration period, and compare non-infilled and infilled products for consistency. The SST  
471 datasets reviewed here are instrumental products and do not assimilate proxy records. Al-  
472 though estimates that synthesize both can be useful (Tingley and Huybers 2010), retaining  
473 independence during calibration remains crucial for intercomparison and bias checking.

474 Once candidates are thinned by practical considerations, it is necessary to assess data quality.  
475 The analysis presented in section 3 shows the importance of choosing the most recent dataset  
476 versions in any family. Typically, older versions of products should be used only alongside their  
477 updated counterparts to aid interpretation of past analyses.

478 Moreover, even the most recent releases can retain period- or region-specific issues, as described  
479 in section 2a with impacts shown in section 3. If a dataset has known problems that could affect the  
480 analysis, it should be excluded. However, if removing such datasets results in too few candidates  
481 for a robust assessment, they should be used with caution, provided their limitations are clearly  
482 acknowledged in the interpretation.

483 Another useful strategy to discriminate among SST products is to evaluate physical consistency  
484 with other quantities such as air temperature, sea-level pressure, precipitation, and cloudiness  
485 (Deser et al. 2010). Yet, this requires understanding how the datasets are constructed and the  
486 assumptions involved. For example, ERSST family’s bias adjustment assumes a relatively stable  
487 difference between SST and nighttime marine air temperatures (Smith and Reynolds 2002); so

488 agreement with those temperatures is not independent support. Similarly, DCSST is adjusted to  
489 be dynamically consistent with its land counterpart DCLSAT (Chan et al. 2023, 2024a). Another  
490 often neglected assumption concerns the spatial covariance embedded in infilling. When records,  
491 especially in data-sparse periods, are infilled by projecting onto prescribed EOF patterns, sub-  
492 sequent EOF analyses will largely recover the imposed covariance structure, rather than reveal  
493 additional information about the underlying variability.

494 In addition to checking robustness across qualifying datasets, results should also be tested against  
495 the estimated uncertainty within each product. This can be done by perturbing the data using the  
496 product’s uncertainty estimates or by analyzing the ensemble. If practical constraints require using  
497 only a subset of an ensemble — such as when running high-resolution AMIP experiments (Chan  
498 et al. 2021) — it is important to understand how the ensemble was constructed so the subset still  
499 represents the intended uncertainty. In HadSST4, for example, the first and second sets of 100  
500 members use different approaches to adjust early SST measurements (Kennedy et al. 2019), so  
501 drawing members from both sub-sets provides a more representative sample.

502 Finally, follow the data-citation instructions provided by journals, which typically require citing  
503 both the dataset and its associated publication, and any additional information requested by dataset  
504 producers. Accurate citation does more than acknowledge the source: it helps dataset providers  
505 secure support for ongoing maintenance and understand how their products are being used, allowing  
506 the datasets to evolve in ways aligned with scientific needs. In turn, this benefits users by increasing  
507 the likelihood that high-quality, regularly updated SST datasets remain available.

#### 508 *b. Where to find more detailed information and updated advice*

509 This paper provides a broad overview of how SST datasets have evolved and their suit-  
510 ability for different climate applications. By design, it cannot cover the full details of in-  
511 dividual products and will freeze at the time of publication. To support users beyond this  
512 snapshot synthesis, we additionally provide a set of NSF NCAR Climate Data Guide pages  
513 (<https://climatedataguide.ucar.edu/>, Schneider et al. 2013) that extend guidance in two  
514 complementary ways.

515 First, dataset-specific pages provide summary information on dataset construction, strengths, and  
516 known limitations, more detailed than this synthesis. Written by the developers or expert users and

517 reviewed by leading climate scientists, these resources, accessible through the web-based selector  
518 tool, help users efficiently evaluate whether any features or issues are critical for their intended  
519 analysis. Once candidate datasets have been identified, there is no substitute for a deep dive into  
520 the linked dataset papers and product user guides for more detailed usage notes and guidance.

521 Second, an SST overview page will be updated to provide an evolving summary of the SST  
522 dataset and evaluation landscape. By tracking newly released updates, methodological advances,  
523 and emerging developments, this page helps ensure that choice and usage guidance remains accurate  
524 and relevant as new and improved datasets become available.

### 525 *c. Anticipated improvements in SST datasets*

526 **Better input data and metadata:** ongoing efforts to rescue historical data (Teleti et al. 2024)  
527 and metadata (Carella et al. 2017) provide valuable independent evidence for evaluating historical  
528 SST biases including those relevant to the early-20th-century cool period and the WWII warm  
529 anomaly. This may be further accelerated by AI-assisted digitization and metadata extraction  
530 (Singh and Middleton 2025). Newly recovered data may also offer opportunities to test the skill of  
531 infilling methods in previously data-sparse regions and periods. Equally importantly, modern data  
532 infrastructure is needed to ensure that both rescued and contemporary observations and metadata  
533 flow efficiently and transparently into permanent archives and SST dataset production — a gap that  
534 currently prevents many recovered measurements from being fully used, including by most of the  
535 SST products discussed here. For satellite-era products, fundamental work on the calibration of  
536 early sensors and SST retrieval methods will also reduce uncertainty and improve stability in the  
537 1980s and 1990s particularly.

538 **Better coverage and finer resolution:** Advances in infilling methodology, including AI ap-  
539 proaches, together with increased computational capacity will support higher spatial and temporal  
540 resolution, with monthly products at 1° or finer as a practical baseline, and 5-day, daily, or sub-  
541 daily products where supported by the observations and practical data-volume constraints. As  
542 these developments progress, the hard boundaries between datasets designed for different pur-  
543 poses are likely to soften, as already seen in COBE-SST3. Feature resolution of satellite-era  
544 products pre-2000 should benefit from efforts (via international co-operation spearheaded by ESA,  
545 <https://ceos.org/news/avhrr-data-recovery/>) to consolidate full-resolution data from early sensors.

546 These higher resolution observations have not been exploited in global SST analyses before, and  
547 provide an opportunity for better understanding changes in ecologically-important shelf sea regions.

548 **Better bias adjustments:** Beyond the pervasive global- and basin-scale biases discussed in section  
549 2a, progress will require pushing bias estimation further toward ship-specific and hence regional  
550 scales, to be enabled by improved metadata such as ship tracking and advanced physical and  
551 statistical models. Meanwhile, broader evaluation using independent sources will be essential  
552 for assessing and refining bias adjustments. Improved methods are also emerging to improve  
553 observational stability in satellite SST records, by extending retrieval methods to be “bias aware”  
554 (Merchant et al. 2020b) and by harmonizing irradiance between satellite platforms prior to retrieval  
555 of SST.

556 **Better structural uncertainty estimates:** As discussed in section 2c, the current practice of  
557 pooling different SST products together does not necessarily provide a comprehensive estimate of  
558 structural uncertainty. As understanding of data artifacts improves, clearly inconsistent products  
559 are recommended to be excluded from certain analyses. This strengthens confidence in the analysis  
560 and metrics of interest, but also narrows the ensemble and reduces its potential to span the full  
561 space of uncertainties that arise across the entire SST production workflow. A more complete  
562 characterization will require decomposing that workflow into its major components — input  
563 selection, quality control, bias adjustment, gridding, and infilling – and sampling alternative  
564 methods and parameter choices within each step. Such a modular approach would help dataset  
565 providers explore the widest range of reasonable choices across each component and ensure that  
566 all known errors and uncertainties are accounted for and fed through to the infilling schemes.  
567 This approach would also lower the barrier for new contributions as novel approaches could be  
568 developed for a single component. For satellite datasets, which are constructed from many trillions  
569 of radiance measurements, modular exploration of structural uncertainty is challenging in terms  
570 of scale and expense because of the large volume, and the community continues to focus on  
571 metrological approaches to exposing, quantifying and correcting effects leading to uncertainty in  
572 SST products (Mittaz et al. 2019).

573 **User-friendly access and data formats:** *In situ* SST datasets are currently dispersed across data  
574 centers, which complicates comparison and analysis. Moving toward common conventions for both  
575 input observations and products, CMIP-style access protocols, regridding and subsetting services

576 such as surftemp.net and cloud-native formats (for example, zarr) will further lower these barriers  
577 and support more scalable, interoperable use of SST products. For satellite SSTs, products have  
578 long been standardized in format, provided with tools, and catalogued through cooperative efforts  
579 of the GHRSSST international science team <https://www.ghrsst.org/>.

580 **Faster-paced innovation:** Delivering the improvements outlined above will require open, stan-  
581 dardized, flexible, and streamlined systems that span data intake, processing, and distribution. Such  
582 infrastructure would better connect data producers and users, broaden participation in development  
583 and evaluation, and ultimately enable users to move from passive recipients of SST products to  
584 active participants in improving both the data and the science derived from them.

## 585 **5. Final words**

586 This paper has shown how careful choice of SST datasets is essential for robust research. Over  
587 time, SST datasets have improved in quality, and their estimates of important measures of variability  
588 have become more consistent. Characterization of dataset uncertainty has also improved, enabling  
589 users to understand the sensitivity of their results to uncertainty within each dataset as well as  
590 between a selection of different datasets. A number of important indicators, including recent and  
591 centennial global trends and the Tropical Pacific trend contrast, show that the most recent SST  
592 dataset versions align more closely with one another, compared with older products. Observational  
593 constraints on future projected surface temperature changes are therefore more robust when using  
594 state-of-the-art datasets than might be inferred from the use of older products.

595 These considerations can be summarized in a set of practical steps to support effective SST  
596 dataset selection and use:

- 597 1. **Use the data-selection tool to identify datasets appropriate for the intended application,**  
598 taking into account record length, residual biases, spatial and temporal resolution, com-  
599 pleteness, uncertainty information, update latency, and specific usage restrictions (e.g., for  
600 commercial use).
- 601 2. **Use this paper and NSF NCAR Climate Data Guide pages to evaluate these candidates,**  
602 gaining an understanding of their construction, strengths, and known limitations.

- 603 3. **Draw on the peer-reviewed dataset literature for the shortlisted products**, including user  
604 guides and methodological papers, to identify issues that may be relevant for the specific  
605 scientific question.
- 606 4. **Wherever possible, analyze the entire uncertainty ensemble and more than one suitable**  
607 **dataset**, so that conclusions can be assessed for robustness to parametric and structural  
608 uncertainty.
- 609 5. **Finally, cite all datasets in accordance with journal and producer guidelines**, including  
610 both the dataset and its associated publications, which supports not only transparent scientific  
611 reuse but also continued maintenance and improvements.

612 Taken together, these practices help ensure that present-day analyses make the best possible  
613 use of available SST datasets. At the same time, continued progress in observational coverage,  
614 data and metadata rescue, understanding of bias and uncertainty, and infrastructure capability will  
615 enable increasingly rapid cycles of improvement. As these advances accelerate, the coexistence  
616 of multiple approaches, each making different methodological choices, will help to better quantify  
617 structural uncertainty, supporting a more robust understanding of past climate change as well as  
618 improved constraints on future projections.

619 *Acknowledgments.* We acknowledge Nick Rayner of the Met Office for her insights on the  
620 HadISST family. D.C. was supported by a UKRI Future Leaders Fellowship (UKRI2360). E.K.  
621 and R.C. were supported by UKRI/NERC via grant NE/Y005589/1. C.D. and N.L. were supported  
622 by the National Center for Atmospheric Research (NCAR), which is sponsored by the National Sci-  
623 ence Foundation under Cooperative Agreement 1852977. C.J.M. was supported by UKRI/NERC  
624 via the National Centre for Earth Observation, grant NE/RO16518/1. C.S. was supported by the  
625 Met Office Hadley Centre Climate Programme, funded by DSIT. P.H. was supported by NSF Grant  
626 2123295. G.G. was supported by U.S. NSF OCE-2122805.

627 *Data availability statement.* All datasets and model output used in this paper are in the public  
628 domain and citation and access information summarized in Table 1.

## 629 **References**

- 630 Abernathey, R. P., and Coauthors, 2021: Cloud-native repositories for big scientific data. *Comput-*  
631 *ing in Science & Engineering*, **23 (2)**, 26–35.
- 632 Allan, R. P., and Coauthors, 2023: Intergovernmental Panel on Climate Change (IPCC). Summary  
633 for policymakers. *Climate change 2021: The physical science basis. Contribution of work-*  
634 *ing group I to the sixth assessment report of the intergovernmental panel on climate change*,  
635 Cambridge University Press, 3–32.
- 636 Beadling, R. L., and Coauthors, 2026: Observational data for next generation climate model  
637 evaluation: Requirements, considerations, and best practices. *BAMS*, **(107)**, E813–E835, URL  
638 <https://doi.org/10.1175/BAMS-D-25-0079.1>.
- 639 Bian, C., Z. Jing, H. Wang, L. Wu, Z. Chen, B. Gan, and H. Yang, 2023: Oceanic mesoscale eddies  
640 as crucial drivers of global marine heatwaves. *Nature Communications*, **14 (1)**, 2970.
- 641 Bottomley, M., C. Folland, J. Hsiung, R. Newell, and D. Parker, 1990: Global ocean surface  
642 temperature atlas (GOSTA). *Meteorological Office, Bracknell, UK*.
- 643 Brasnett, B., 2008: The impact of satellite retrievals in a global sea-surface-temperature analysis.  
644 *Quarterly Journal of the Royal Meteorological Society*, **134 (636)**, 1745–1760.
- 645 Brönnimann, S., J. Luterbacher, J. Staehelin, T. M. Svendby, G. Hansen, and T. Svenøe, 2004:  
646 Extreme climate of the global troposphere and stratosphere in 1940–42 related to El Niño. *Nature*,  
647 **431 (7011)**, 971–974, doi:10.1038/nature02982, URL <http://dx.doi.org/10.1038/nature02982>.
- 648 Byrne, H., R. Seager, and J. E. Smerdon, 2025: CMIP6 models cannot capture long-term forced  
649 changes in the tropical Pacific sea surface temperature gradient. *Nature Communications*.
- 650 Carella, G., E. C. Kent, and D. I. Berry, 2017: A probabilistic approach to ship voyage reconstruc-  
651 tion in ICOADS. *International Journal of Climatology*, **37 (5)**, 2233–2247.
- 652 Cavalieri, D. J., C. L. Parkinson, N. DiGirolamo, and A. Ivanoff, 2011: Intersensor calibration  
653 between F13 SSMI and F17 SSMIS for global sea ice data records. *IEEE Geoscience and Remote*  
654 *Sensing Letters*, **9 (2)**, 233–236.

655 Chan, D., 2021: Combining statistical, physical, and historical evidence to improve historical  
656 sea-surface temperature records. Ph.D. thesis, Harvard University.

657 Chan, D., S. C. Chan, J. T. Siddons, A. Cable, R. C. Cornes, E. C. Kent, G. Gebbie, and P. Huybers,  
658 2026: DCENT-I: A globally infilled extension of the Dynamically Consistent ENsemble of  
659 Temperature dataset. *Geoscience Data Journal*, **In press**.

660 Chan, D., G. Gebbie, and P. Huybers, 2023: Global and regional discrepancies between early 20th  
661 century coastal air and sea-surface temperature detected by a coupled energy-balance analysis.  
662 *Journal of Climate*, **36 (7)**, 2205–2220.

663 Chan, D., G. Gebbie, and P. Huybers, 2024b: An improved ensemble of land-surface air temper-  
664 atures since 1880 using revised pair-wise homogenization algorithms accounting for autocorre-  
665 lation. *Journal of Climate*.

666 Chan, D., G. Gebbie, and P. Huybers, 2025: Re-evaluating historical sea surface temperature  
667 data sets: Insights from the diurnal cycle, coral proxy data, and radiative forcing. *Geophysical*  
668 *Research Letters*, **52 (13)**, e2025GL116615.

669 Chan, D., G. Gebbie, P. Huybers, and E. C. Kent, 2024a: A Dynamically Consistent ENsemble of  
670 Temperature at the Earth surface since 1850 from the DCENT dataset. *Scientific Data*, **11 (1)**,  
671 953.

672 Chan, D., and P. Huybers, 2019: Systematic differences in bucket sea surface temperature measure-  
673 ments among nations identified using a linear-mixed-effect method. *Journal of Climate*, **32 (9)**,  
674 2569–2589.

675 Chan, D., and P. Huybers, 2021: Correcting observational biases in sea surface temperature  
676 observations removes anomalous warmth during World War II. *Journal of Climate*, **34 (11)**,  
677 4585–4602.

678 Chan, D., E. C. Kent, D. I. Berry, and P. Huybers, 2019: Correcting datasets leads to more  
679 homogeneous early-twentieth-century sea surface warming. *Nature*, **571 (7765)**, 393.

680 Chan, D., G. A. Vecchi, W. Yang, and P. Huybers, 2021: Improved simulation of 19th-and 20th-  
681 century North Atlantic hurricane frequency after correcting historical sea surface temperatures.  
682 *Science Advances*, **7 (26)**, eabg6931.

683 Chin, T. M., J. Vazquez-Cuervo, and E. M. Armstrong, 2017: A multi-scale high-resolution  
684 analysis of global sea surface temperature. *Remote sensing of environment*, **200**, 154–169.

685 Delworth, T. L., and T. R. Knutson, 2000: Simulation of early 20th century global warming.  
686 *Science*, **287 (5461)**, 2246–2250.

687 Deser, C., A. S. Phillips, and M. A. Alexander, 2010: Twentieth century tropical sea surface  
688 temperature trends revisited. *Geophysical Research Letters*, **37 (10)**.

689 Deser, C., and Coauthors, 2012: ENSO and Pacific decadal variability in the Community Climate  
690 System Model version 4. *Journal of Climate*, **25 (8)**, 2622–2651.

691 Dong, Y., A. G. Pauling, S. Sadai, and K. C. Armour, 2022: Antarctic ice-sheet meltwater reduces  
692 transient warming and climate sensitivity through the sea-surface temperature pattern effect.  
693 *Geophysical Research Letters*, **49 (24)**, e2022GL101 249.

694 Dong, Y., L. M. Polvani, and D. B. Bonan, 2023: Recent multi-decadal southern ocean surface  
695 cooling unlikely caused by southern annular mode trends. *Geophysical Research Letters*, **50 (23)**,  
696 e2023GL106 142.

697 Embury, O., and C. J. Merchant, 2012: A reprocessing for climate of sea surface temperature from  
698 the along-track scanning radiometers: A new retrieval scheme. *Remote Sensing of Environment*,  
699 **116**, 47–61, doi:10.1016/j.rse.2010.11.020, URL <http://dx.doi.org/10.1016/j.rse.2010.11.020>.

700 Embury, O., and Coauthors, 2024: Satellite-based time-series of sea-surface temperature since  
701 1980 for climate applications. *Scientific Data*, **11 (1)**, 326.

702 Eyring, V., S. Bony, G. A. Meehl, C. A. Senior, B. Stevens, R. J. Stouffer, and K. E. Taylor, 2016:  
703 Overview of the Coupled Model Intercomparison Project Phase 6 (CMIP6) experimental design  
704 and organization. *Geoscientific Model Development*, **9 (5)**, 1937–1958.

705 Eyring, V., and Coauthors, 2023: *Human influence on the climate system, Chapter 3 in Climate*  
706 *Change 2021: The Physical Science Basis. Contribution of Working Group I to the Sixth*  
707 *Assessment Report of the Intergovernmental Panel on Climate Change [Masson-Delmotte, V., P.*  
708 *Zhai, A. Pirani, S.L. Connors, C. Péan, S. Berger, N. Caud, Y. Chen, L. Goldfarb, M.I. Gomis, M.*

709 Huang, K. Leitzell, E. Lonnoy, J.B.R. Matthews, T.K. Maycock, T. Waterfield, O. Yelekçi, R. Yu,  
710 and B. Zhou (eds.)], 423–552. Cambridge University Press, doi:10.1017/9781009157896.005.

711 Fiedler, E. K., and Coauthors, 2019: Intercomparison of long-term sea surface temperature analyses  
712 using the GHR SST Multi-Product Ensemble (GMPE) system. *Remote Sensing of Environment*,  
713 **222**, 18–33, doi:10.1016/j.rse.2018.12.015, URL <http://dx.doi.org/10.1016/j.rse.2018.12.015>.

714 Folland, C., and D. Parker, 1995: Correction of instrumental biases in historical sea surface  
715 temperature data. *Quarterly Journal of the Royal Meteorological Society*, **121 (522)**, 319–367.

716 Folland, C. K., D. Parker, and F. Kates, 1984: Worldwide marine temperature fluctuations 1856–  
717 1981. *Nature*, **310 (5979)**, 670–673.

718 Forget, G., J.-M. Campin, P. Heimbach, C. Hill, R. Ponte, and C. Wunsch, 2015: Ecco version  
719 4: An integrated framework for non-linear inverse modeling and global ocean state estimation.  
720 *Geoscientific Model Development*, **8 (10)**, 3071–3104.

721 Freeman, E., and Coauthors, 2017: ICOADS Release 3.0: a major update to the historical marine  
722 climate record. *International Journal of Climatology*, **37 (5)**, 2211–2232.

723 Gottschalk, B., 2017: Global surface temperature trends and the effect of World War II. URL  
724 <https://arxiv.org/abs/1703.09281>, 1703.09281.

725 Gregory, J. M., and Coauthors, 2024: A new conceptual model of global ocean heat uptake.  
726 *Climate Dynamics*, **62 (3)**, 1669–1713.

727 Hegerl, G. C., S. Brönnimann, A. Schurer, and T. Cowan, 2018: The early 20th century warming:  
728 Anomalies, causes, and consequences. *Wiley Interdisciplinary Reviews: Climate Change*, **9 (4)**,  
729 e522.

730 Hersbach, H., and Coauthors, 2020: The ERA5 global reanalysis. *Quarterly Journal of the Royal*  
731 *Meteorological Society*, **146 (730)**, 1999–2049, doi:10.1002/qj.3803, URL [http://dx.doi.org/10.](http://dx.doi.org/10.1002/qj.3803)  
732 [1002/qj.3803](http://dx.doi.org/10.1002/qj.3803).

733 Hirahara, S., M. Ishii, and Y. Fukuda, 2014: Centennial-scale sea surface temperature analysis and  
734 its uncertainty. *Journal of Climate*, **27 (1)**, 57–75.

- 735 Huang, B., C. Liu, V. Banzon, E. Freeman, G. Graham, B. Hankins, T. Smith, and H.-M. Zhang,  
736 2021: Improvements of the daily optimum interpolation sea surface temperature (DOISST)  
737 version 2.1. *Journal of Climate*, **34 (8)**, 2923–2939.
- 738 Huang, B., and Coauthors, 2015: Extended reconstructed sea surface temperature version 4  
739 (ERSST.v4). Part I: Upgrades and intercomparisons. *Journal of Climate*, **28 (3)**, 911–930.
- 740 Huang, B., and Coauthors, 2017: Extended reconstructed sea surface temperature, version 5  
741 (ERSSTv5): upgrades, validations, and intercomparisons. *Journal of Climate*, **30 (20)**, 8179–  
742 8205.
- 743 Huang, B., and Coauthors, 2025: Extended reconstructed sea surface temperature, version 6  
744 (ERSSTv6). part I: an artificial neural network approach. *Journal of Climate*, **38 (4)**, 1105–1121.
- 745 Hurrell, J. W., J. J. Hack, D. Shea, J. M. Caron, and J. Rosinski, 2008: A new sea surface temperature  
746 and sea ice boundary dataset for the community atmosphere model. *Journal of Climate*, **21 (19)**,  
747 5145–5153, doi:10.1175/2008jcli2292.1, URL <http://dx.doi.org/10.1175/2008JCLI2292.1>.
- 748 Ishii, M., A. Nishimura, S. Yasui, and S. Hirahara, 2025: Historical high-resolution daily SST  
749 analysis (COBE-SST3) with consistency to monthly land surface air temperature. *Journal of the*  
750 *Meteorological Society of Japan. Ser. II*, **103 (1)**, 17–44.
- 751 Ishii, M., A. Shouji, S. Sugimoto, and T. Matsumoto, 2005: Objective analyses of sea-surface  
752 temperature and marine meteorological variables for the 20th century using ICOADS and the  
753 Kobe collection. *International Journal of Climatology*, **25 (7)**, 865–879.
- 754 Jean-Michel, L., and Coauthors, 2021: The Copernicus global 1/12 oceanic and sea ice GLORYS12  
755 reanalysis. *Frontiers in Earth Science*, **9**, 698 876.
- 756 Jones, P. D., T. M. Wigley, and P. B. Wright, 1986: Global temperature variations between 1861  
757 and 1984. *Nature*, **322 (6078)**, 430–434.
- 758 Kang, S. M., Y. Shin, H. Kim, S.-P. Xie, and S. Hu, 2023: Disentangling the mechanisms of  
759 equatorial pacific climate change. *Science Advances*, **9 (19)**, eadf5059.

- 760 Kaplan, A., M. A. Cane, Y. Kushnir, A. C. Clement, M. B. Blumenthal, and B. Rajagopalan,  
761 1998: Analyses of global sea surface temperature 1856–1991. *Journal of Geophysical Research:*  
762 *Oceans*, **103 (C9)**, 18 567–18 589.
- 763 Kaplan, A., Y. Kushnir, M. A. Cane, and M. B. Blumenthal, 1997: Reduced space optimal analysis  
764 for historical data sets: 136 years of Atlantic sea surface temperatures. *Journal of Geophysical*  
765 *Research: Oceans*, **102 (C13)**, 27 835–27 860.
- 766 Karl, T. R., and Coauthors, 2015: Possible artifacts of data biases in the recent global surface  
767 warming hiatus. *Science*, **348 (6242)**, 1469–1472.
- 768 Kennedy, J., N. Rayner, C. Atkinson, and R. Killick, 2019: An Ensemble Data Set of Sea Surface  
769 Temperature Change From 1850: The Met Office Hadley Centre HadSST. 4.0.0.0 Data Set.  
770 *Journal of Geophysical Research: Atmospheres*, **124 (14)**, 7719–7763.
- 771 Kennedy, J., N. Rayner, R. Smith, D. Parker, and M. Saunby, 2011a: Reassessing biases and other  
772 uncertainties in sea surface temperature observations measured in situ since 1850: 1. measure-  
773 ment and sampling uncertainties. *Journal of Geophysical Research: Atmospheres*, **116 (D14)**.
- 774 Kennedy, J., N. Rayner, R. Smith, D. Parker, and M. Saunby, 2011b: Reassessing biases and other  
775 uncertainties in sea surface temperature observations measured in situ since 1850: 2. biases and  
776 homogenization. *Journal of Geophysical Research: Atmospheres*, **116 (D14)**.
- 777 Kennedy, J. J., 2014: A review of uncertainty in in situ measurements and data sets of sea surface  
778 temperature. *Reviews of Geophysics*, **52 (1)**, 1–32.
- 779 Kent, E. C., and J. J. Kennedy, 2021: Historical estimates of surface marine temperatures. *Annual*  
780 *Review of Marine Science*, **13**, 283–311.
- 781 Kent, E. C., N. A. Rayner, D. I. Berry, M. Saunby, B. I. Moat, J. J. Kennedy, and D. E. Parker, 2013:  
782 Global analysis of night marine air temperature and its uncertainty since 1880: The HadNMAT2  
783 data set. *Journal of Geophysical Research: Atmospheres*, **118 (3)**, 1281–1298.
- 784 Kent, E. C., and P. K. Taylor, 2006: Toward estimating climatic trends in SST. Part I: Methods of  
785 measurement. *Journal of Atmospheric and Oceanic Technology*, **23 (3)**, 464–475.

786 Knight, J. R., C. K. Folland, and A. A. Scaife, 2006: Climate impacts of the Atlantic multidecadal  
787 oscillation. *Geophysical Research Letters*, **33** (17).

788 Kosaka, Y., and Coauthors, 2024: The JRA-3Q Reanalysis. *Journal of the Meteorological Society*  
789 *of Japan. Ser. II*, **102** (1), 49–109, doi:10.2151/jmsj.2024-004, URL [http://dx.doi.org/10.2151/  
790 jmsj.2024-004](http://dx.doi.org/10.2151/jmsj.2024-004).

791 Lee, S., M. L’Heureux, A. T. Wittenberg, R. Seager, P. A. O’Gorman, and N. C. John-  
792 son, 2022: On the future zonal contrasts of equatorial Pacific climate: Perspectives from  
793 observations, simulations, and theories. *npj Climate and Atmospheric Science*, **5** (1), doi:  
794 10.1038/s41612-022-00301-2, URL <http://dx.doi.org/10.1038/s41612-022-00301-2>.

795 McPhaden, M. J., S. E. Zebiak, and M. H. Glantz, 2006: ENSO as an integrating concept in earth  
796 science. *Science*, **314** (5806), 1740–1745.

797 Menemenlis, S., G. A. Vecchi, W. Yang, and Coauthors, 2025: Consequential differences in  
798 satellite-era sea surface temperature trends across datasets. *Nature Climate Change*, **15**, 897–  
799 903, doi:10.1038/s41558-025-02362-6, URL <https://doi.org/10.1038/s41558-025-02362-6>.

800 Merchant, C., P. Le Borgne, A. Marsouin, and H. Roquet, 2008a: Optimal estimation of sea  
801 surface temperature from split-window observations. *Remote Sensing of Environment*, **112** (5),  
802 2469–2484, doi:10.1016/j.rse.2007.11.011, URL <http://dx.doi.org/10.1016/j.rse.2007.11.011>.

803 Merchant, C., and Coauthors, 2008b: Deriving a sea surface temperature record suitable for climate  
804 change research from the along-track scanning radiometers. *Advances in Space Research*, **41** (1),  
805 1–11.

806 Merchant, C. J., A. R. Harris, M. J. Murray, and A. M. Závody, 1999: Toward the elimination  
807 of bias in satellite retrievals of sea surface temperature: 1. theory, modeling and interalgorithm  
808 comparison. *Journal of Geophysical Research: Oceans*, **104** (C10), 23 565–23 578, doi:10.  
809 1029/1999jc900105, URL <http://dx.doi.org/10.1029/1999JC900105>.

810 Merchant, C. J., S. Saux-Picart, and J. Waller, 2020a: Bias correction and covariance parameters  
811 for optimal estimation by exploiting matched in-situ references. *Remote Sensing of Environ-*  
812 *ment*, **237**, 111 590, doi:10.1016/j.rse.2019.111590, URL [http://dx.doi.org/10.1016/j.rse.2019.  
111590](http://dx.doi.org/10.1016/j.rse.2019.<br/>813 111590).

814 Merchant, C. J., S. Saux-Picart, and J. Waller, 2020b: Bias correction and covariance parameters  
815 for optimal estimation by exploiting matched in-situ references. *Remote Sensing of Environment*,  
816 **237**, 111–159.

817 Mittaz, J., C. J. Merchant, and E. R. Woolliams, 2019: Applying principles of metrology to  
818 historical earth observations from satellites. *Metrologia*, **56** (3), 032–002.

819 Oliver, E. C., J. A. Benthuisen, S. Darmaraki, M. G. Donat, A. J. Hobday, N. J. Holbrook, R. W.  
820 Schlegel, and A. Sen Gupta, 2021: Marine heatwaves. *Annual Review of Marine Science*, **13** (1),  
821 313–342.

822 Pfeiffer, M., J. Zinke, W.-C. Dullo, D. Garbe-Schönberg, M. Latif, and M. Weber, 2017: Indian  
823 ocean corals reveal crucial role of world war ii bias for twentieth century warming estimates.  
824 *Scientific Reports*, **7** (1), 14–434.

825 Rayner, N., P. Brohan, D. Parker, C. Folland, J. Kennedy, M. Vanicek, T. Ansell, and S. Tett, 2006:  
826 Improved analyses of changes and uncertainties in sea surface temperature measured in situ since  
827 the mid-nineteenth century: the HadSST2 dataset. *Journal of Climate*, **19** (3), 446–469.

828 Rayner, N., D. E. Parker, E. Horton, C. Folland, L. Alexander, D. Rowell, E. Kent, and A. Kaplan,  
829 2003: Global analyses of sea surface temperature, sea ice, and night marine air temperature  
830 since the late nineteenth century. *Journal of Geophysical Research: Atmospheres*, **108** (D14).

831 Reynolds, R. W., 1993: Impact of Mount Pinatubo aerosols on satellite-derived sea surface  
832 temperatures. *Journal of Climate*, **6** (4), 768–774.

833 Reynolds, R. W., D. B. Chelton, J. Roberts-Jones, M. J. Martin, D. Menemenlis, and C. J.  
834 Merchant, 2013: Objective determination of feature resolution in two sea surface temperature  
835 analyses. *Journal of Climate*, **26** (8), 2514–2533, doi:10.1175/jcli-d-12-00787.1, URL <http://dx.doi.org/10.1175/JCLI-D-12-00787.1>.

836

837 Reynolds, R. W., N. A. Rayner, T. M. Smith, D. C. Stokes, and W. Wang, 2002: An improved in  
838 situ and satellite SST analysis for climate. *Journal of Climate*, **15** (13), 1609–1625.

839 Reynolds, R. W., T. M. Smith, C. Liu, D. B. Chelton, K. S. Casey, and M. G. Schlax, 2007:  
840 Daily high-resolution-blended analyses for sea surface temperature. *Journal of Climate*, **20** (22),  
841 5473–5496.

- 842 Rohde, R. A., and Z. Hausfather, 2020: The Berkeley Earth land/ocean temperature record. *Earth*  
843 *System Science Data*, **12** (4), 3469–3479.
- 844 Sandford, C., and N. Rayner, 2026: Addressing the World War 2 Warm Anomaly in HadSST.4.2.0.0.  
845 *International Journal of Climatology*, URL <https://doi.org/10.1002/joc.70388>.
- 846 Schneider, D. P., C. Deser, and T. Fan, 2015: Comparing the impacts of tropical sst variability  
847 and polar stratospheric ozone loss on the southern ocean westerly winds. *Journal of Climate*,  
848 **28** (23), 9350–9372.
- 849 Schneider, D. P., C. Deser, J. Fasullo, and K. E. Trenberth, 2013: Climate data guide spurs discovery  
850 and understanding. *Eos, Transactions American Geophysical Union*, **94** (13), 121–122.
- 851 Seager, R., M. Cane, N. Henderson, D.-E. Lee, R. Abernathey, and H. Zhang, 2019: Strengthening  
852 tropical pacific zonal sea surface temperature gradient consistent with rising greenhouse gases.  
853 *Nature Climate Change*, **9** (7), 517–522.
- 854 Seviour, W., and Coauthors, 2019: The southern ocean sea surface temperature response to ozone  
855 depletion: A multimodel comparison. *Journal of Climate*, **32** (16), 5107–5121.
- 856 Sherwood, S. C., and Coauthors, 2020: An assessment of Earth’s climate sensitivity using multiple  
857 lines of evidence. *Reviews of Geophysics*, **58** (4), e2019RG000678.
- 858 Singh, L. G., and S. E. Middleton, 2025: Data rescue of historical tables through semi-supervised  
859 table structure recognition. *International Journal on Document Analysis and Recognition (IJ-*  
860 *DAR)*, 1–17.
- 861 Sippel, S., and Coauthors, 2024: Early-twentieth-century cold bias in ocean surface temperature  
862 observations. *Nature*, **635** (8039), 618–624.
- 863 Smith, T. M., R. E. Livezey, and S. S. Shen, 1998: An improved method for analyzing sparse  
864 and irregularly distributed SST data on a regular grid: The tropical Pacific Ocean. *Journal of*  
865 *Climate*, **11** (7), 1717–1729.
- 866 Smith, T. M., and R. W. Reynolds, 2002: Bias corrections for historical sea surface temperatures  
867 based on marine air temperatures. *Journal of Climate*, **15** (1), 73–87.

- 868 Smith, T. M., R. W. Reynolds, T. C. Peterson, and J. Lawrimore, 2008: Improvements to NOAA's  
869 historical merged land–ocean surface temperature analysis (1880–2006). *Journal of Climate*,  
870 **21 (10)**, 2283–2296.
- 871 Teleti, P., E. Hawkins, and K. R. Wood, 2024: Digitizing weather observations from World War II  
872 US naval ship logbooks. *Geoscience Data Journal*, **11 (3)**, 314–329.
- 873 Thompson, D. W., J. J. Kennedy, J. M. Wallace, and P. D. Jones, 2008: A large discontinuity in  
874 the mid-twentieth century in observed global-mean surface temperature. *Nature*, **453 (7195)**,  
875 646–649.
- 876 Thorne, P. W., D. E. Parker, J. R. Christy, and C. A. Mears, 2005: Uncertainties in climate trends:  
877 Lessons from upper-air temperature records. *Bulletin of the American Meteorological Society*,  
878 **86 (10)**, 1437–1442.
- 879 Tingley, M. P., and P. Huybers, 2010: A Bayesian algorithm for reconstructing climate anomalies in  
880 space and time. Part I: Development and applications to paleoclimate reconstruction problems.  
881 *Journal of Climate*, **23 (10)**, 2759–2781.
- 882 Trenberth, K. E., 1997: The definition of El Niño. *Bulletin of the American Meteorological Society*,  
883 **78 (12)**, 2771–2778.
- 884 Trenberth, K. E., and D. J. Shea, 2006: Atlantic hurricanes and natural variability in 2005.  
885 *Geophysical Research Letters*, **33 (12)**.
- 886 Watanabe, M., J.-L. Dufresne, Y. Kosaka, T. Mauritsen, and H. Tatebe, 2021: Enhanced warming  
887 constrained by past trends in equatorial Pacific sea surface temperature gradient. *Nature Climate*  
888 *Change*, **11 (1)**, 33–37.
- 889 Wittenberg, A. T., 2009: Are historical records sufficient to constrain ENSO simulations? *Geo-*  
890 *physical Research Letters*, **36 (12)**.
- 891 Worsfold, M., S. Good, C. Atkinson, and O. Embury, 2024: Presenting a long-term, reprocessed  
892 dataset of global sea surface temperature produced using the OSTIA system. *Remote Sensing*,  
893 **16 (18)**, 3358.

894 Yang, C., and Coauthors, 2021: Sea surface temperature intercomparison in the framework of  
895 the Copernicus Climate Change Service (C3S). *Journal of Climate*, **34** (13), 5257–5283, doi:  
896 10.1175/jcli-d-20-0793.1, URL <http://dx.doi.org/10.1175/JCLI-D-20-0793.1>.